Design of Structured Controllers for Linear Time-Delay Systems

Wim Michiels

Abstract We present an overview of control design methods for linear time-delay systems, which are grounded in matrix theory and numerical linear algebra techniques, such as eigenvalue computations, solving Lyapunov matrix equations, eigenvalue perturbation theory and eigenvalue optimization. The methods are particularly suitable for the design of structured controllers, as they rely on a direct optimization of stability, robustness and performance indicators as a function of controller or design parameters. Several illustrations complete the presentation.

1 Introduction

We consider the system

$$\begin{cases} \dot{x}(t) = A_0 x(t) + \sum_{i=1}^{m} A_i x(t-\tau_i) + B\zeta(t), \\ \eta(t) = Cx(t) + D\zeta(t-\tau_0), \end{cases} \tag{1}$$

where $x(t) \in \mathbb{C}^n$ is the state variable at time t, $\zeta(t) \in \mathbb{C}^{n_\zeta}$ is the input and $\eta(t) \in \mathbb{C}^{n_\eta}$ is the output at time t, and τ_i, $i = 0, \ldots, m$, represent time-delays. We assume that the state delays are ordered such that $0 < \tau_1 < \cdots < \tau_m$. The input is not assumed to be delayed, yet input-output delays can be taken into account in the models addressed in Sect. 5.

It is well known that the solutions of (1), with $\zeta \equiv 0$, satisfy a spectrum determined growth property, in the sense that their asymptotic behavior and stability properties

This work was supported by the project C14/17/072 of the KU Leuven Research Council, by the project G092721N of the Research Foundation-Flanders (FWO - Vlaanderen), and by the project UCoCoS, funded by the European Unions Horizon 2020 research and innovation programme under the Marie Sklodowska-Curie Grant Agreement No 675080.

W. Michiels (✉)
Department of Computer Science, KU Leuven, Heverlee, Belgium
e-mail: Wim.Michiels@cs.kuleuven.be

D. Breda (ed.), *Controlling Delayed Dynamics*, CISM International Centre for Mechanical Sciences 604, https://doi.org/10.1007/978-3-031-01129-0_8

are determined by the location of the characteristic roots, see Hale and Verduyn Lunel (1993), compare also with Breda (2023). The latter appear among the solutions of the nonlinear eigenvalue problem

$$\left(\lambda I - A_0 - \sum_{i=1}^{m} A_i e^{-\lambda \tau_i}\right) v = 0, \ v \in \mathbb{C}^n, \ v \neq 0. \tag{2}$$

For example the null solution of (1), with zero input, is exponentially stable if and only if all its characteristic roots are confined to the open left half plane (Niculescu 2001; Gu et al. 2003). In such a case, we call system (1) internally exponentially stable.

As a common approach in the domain of robust control, we assume that input ζ and output η are defined in such a way that performance and robustness requirements for the system can be expressed in terms of norms of the associated transfer function $G : \mathbb{C} \to \mathbb{C}^{n_\eta \times n_\zeta}$,

$$G(\lambda) := C \left(\lambda I - A_0 - \sum_{i=1}^{m} A_i e^{-\lambda \tau_i}\right)^{-1} B + D e^{-\lambda \tau_0}, \tag{3}$$

which corresponds to the Laplace transform of the impulse response h of the system. Important measures are the $\mathcal{H}_2$ and $\mathcal{H}_\infty$ norm of the input-output map of the system (Zhou et al. 1995). For an internally exponentially stable system, the $\mathcal{H}_2$ norm is defined as

$$\|G\|_{\mathcal{H}_2} := \sqrt{\int_0^\infty \operatorname{tr}\left(h(t)^H h(t)\right) \mathrm{d}t},$$

which, by Parseval's relation, can also be expressed as

$$\|G\|_{\mathcal{H}_2} = \sqrt{\frac{1}{2\pi} \int_{-\infty}^{\infty} \operatorname{tr}\left(G(\mathrm{i}\omega)^H G(\mathrm{i}\omega)\right) \mathrm{d}\omega}. \tag{4}$$

The $\mathcal{H}_2$ norm is particularly suitable to quantify the effects of additive perturbations to the differential equation on the deviation from the equilibrium, as it can be interpreted as the trace of the covariance matrix of the output, when the system input consists of white noise. The $\mathcal{H}_\infty$ norm, on its turn, is equal to the peak gain of the transfer function in the closed right half plane. Once again under assumption of internal exponential stability, it can be defined by the expression

$$\|G\|_{\mathcal{H}_\infty} := \sup_{\omega \in \mathbb{R}} \sigma_1(G(\mathrm{i}\omega)),$$

where $\sigma_1(\cdot)$ denotes the largest singular value. In the time-domain the $\mathcal{H}_\infty$ norm can be interpreted as the induced $\mathcal{L}_2$-norm from input ζ to output η, when considered

as functions on the interval $[0, \infty)$, that is $\|G\|_{\mathcal{H}_\infty} = \max_{u \not\equiv 0} \frac{\|y\|_{\mathcal{L}_2}}{\|u\|_{\mathcal{L}_2}}$, emphasizing its role in assessing the disturbance rejection of a dynamical system. In addition, many robustness criteria for stability against perturbations to system model (1) can be expressed in terms of the reciprocal of the $\mathcal{H}_\infty$ norm of an appropriately defined transfer function. For example, considering complex valued perturbations δA_i on matrices A_i, $i = 0, \ldots, m$, in (1), whose size is measured by

$$\|(\delta A_0, \ldots, \delta A_m)\|_{\text{glob}} := \left\| \begin{bmatrix} w_0 \|\delta A_0\|_2 \\ \vdots \\ w_m \|\delta A_m\|_2 \end{bmatrix} \right\|_\infty,$$

where numbers $w_i \in \mathbb{R}_0^+ \cup \{\infty\}$[1] are weights associated to the different matrix perturbations, the associated stability radius

$$r_{\mathbb{C}}(\|\cdot\|_{\text{glob}}) := \inf \Big\{ \|(\delta A_0, \ldots, \delta A_m)\|_{\text{glob}} : \ \delta A_i \in \mathbb{C}^{n\times n}, 0 \le i \le m, \text{ and } \dot{x}(t) = (A_0 + \delta A_0)x(t) + \textstyle\sum_{i=1}^m (A_i + \delta A_i)x(t - \tau_i)) \text{ is not exponentially stable} \Big\}$$

can be expressed as

$$r_{\mathbb{C}}(\|\cdot\|_{\text{glob}}) = \left\{ \left\| \left(\mathrm{i}\omega I - A_0 - \sum_{i=1}^m A_i e^{-\mathrm{i}\omega\tau_i} \right)^{-1} \right\|_{\mathcal{H}_\infty} \sum_{i=0}^m \frac{1}{w_i} \right\}^{-1},$$

see Michiels and Niculescu (2014). It should be noticed that

$$\|(\delta A_0, \ldots, \delta A_m)\|_{\text{glob}} < 1 \ \Leftrightarrow \ \|\delta A_i\|_2 < \frac{1}{w_i}, 0 \le i \le m.$$

The above result can be extended by exploiting structured, real valued perturbations, see, e.g., Borgioli and Michiels (2020), Borgioli et al. (2019), where the $\mathcal{H}_\infty$ framework is generalized to the μ-framework (Zhou et al. 1995). We note that Borgioli et al. (2019) also considers bounded perturbations on the delays. Finally, the system norms can also be used in the context of structure preserving model reduction. Denoting by $\tilde{G}$ the transfer function of a reduced model for (1) of the form

$$\hat{G}(\mathrm{i}\omega) = \hat{C} \left(\lambda I - \sum_{i=0}^m \hat{A}_i e^{-\lambda\tau_i} \right)^{-1} \hat{B} + D e^{-\lambda\tau_0}, \quad \hat{A}_i \in \mathbb{C}^{k\times k}, \ i = 0, \ldots, m,$$

assuming n large and $k \ll n$, the matrices of the reduced model could be determined by minimizing

$$\|G - \tilde{G}\|_{\mathcal{H}_2}, \text{ or } \|G - \tilde{G}\|_{\mathcal{H}_\infty},$$

[1] $\mathbb{R}_0^+$ denotes the set of strictly positive real numbers.

see Gomez et al. (2019), Pontes Duff et al. (2018). Here we can express the mismatch between the transfer functions in the form of a standard transfer function, namely

$$G(\mathrm{i}\omega) - \hat{G}(\mathrm{i}\omega) = [C \ -\hat{C}] \times \left(\mathrm{i}\omega \begin{bmatrix} I_n & 0 \\ 0 & I_k \end{bmatrix} - \sum_{i=0}^{m} \begin{bmatrix} A_i & 0 \\ 0 & \hat{A}_i \end{bmatrix} e^{-\mathrm{i}\omega\tau_i} \right)^{-1} \begin{bmatrix} B \\ \hat{B} \end{bmatrix},$$

enabling tools for optimizing system or controller parameters.

The structure of the chapter is as follows. In Sect. 2 we present some numerical methods for the computation of the rightmost characteristic roots of (1) and for the computation of the $\mathcal{H}_2$ and $\mathcal{H}_\infty$ norm of transfer function (3). These analysis tools are at the basis of the controller synthesis methods discussed in Sect. 3. There we assume that the system matrices in (1) depend on a finite number of parameters, which may originate from the parametrization of a controller (hence, system (1) may correspond already to the so-called *closed-loop* system). The stabilization problem and the optimization of the $\mathcal{H}_2$ and $\mathcal{H}_\infty$ norm of (3) are addressed. The approach is inspired by controller synthesis methods for finite-dimensional linear time-invariant systems which rely on eigenvalue optimization, as for instance implemented in the package HIFOO (Burke et al. 2006). These methods have proven very useful for synthesis problems where the controller is constrained or its order (dimension) is smaller than the dimension of the plant. They are particularly powerful for time-delay systems, because any design problem involving the determination of a finite number of parameters can be interpreted as a reduced-order control design problem due to the infinite dimension of the system, and they constitute an important component of the established eigenvalue based framework for time-delay systems (Michiels and Niculescu 2014; Michiels 2019). In Sect. 4 we illustrate the flexibility of the approach in two complementary directions, by incorporating pole location constraints in the stabilization procedure, and by synthesizing a proportional-retarded controller optimizing the $\mathcal{H}_2$ norm of the system, respectively. In Sect. 5 we briefly address extensions of the approach towards delay differential algebraic equation models, which can also describe systems of neutral type. Finally, in Sect. 6 we present some concluding remarks.

2 Solving Analysis Problems

We start with the reformulation of (1) as an infinite-dimensional linear system in a standard state space representation, based on Curtain and Zwart (1995), because the interplay between the two representations has played an important role in the development of computational tools. Consider the Hilbert space $X := \mathbb{C}^n \times \mathcal{L}_2([-\tau_m, 0], \mathbb{C}^n)$, equipped with the inner product

$$< (y_0, y_1), (z_0, z_1) >_X = < y_0, z_0 >_{\mathbb{C}^n} + < y_1, z_1 >_{\mathcal{L}_2},$$

and denote by $AC([-\tau_m, 0], \mathbb{C}^n)$ the space of absolutely continuous functions from $[-\tau_m, 0]$ to $\mathbb{C}^n$. Let $\mathcal{A} : X \to X$ be the derivative operator defined by

$$\mathcal{D}(\mathcal{A}) := \{z = (z_0, z_1) \in X : z_1 \in AC([-\tau_m, 0], \mathbb{C}^n),\ z_0 = z_1(0)\},$$
$$\mathcal{A}z = \left(A_0 z_0 + \sum_{i=1}^{m} A_i z_1(-\tau_i)\right), \quad z \in \mathcal{D}(\mathcal{A}),$$

and let the operators $\mathcal{B} : \mathbb{C}^{n_\zeta} \to X$ and $\mathcal{C} : X \to \mathbb{C}^{n_\eta}$ be given by

$$\begin{array}{ll} \mathcal{B}\zeta := (B\zeta, 0), & \zeta \in \mathbb{C}^{n_\zeta}, \\ \mathcal{C}z := Cz_0, & z = (z_0, z_1) \in X. \end{array}$$

We can now rewrite system (1) as

$$\begin{cases} \dot{\Xi}(t) = \mathcal{A}\Xi(t) + \mathcal{B}\zeta(t), \\ \eta(t) \ = \mathcal{C}\Xi(t) + D\zeta(t - \tau_0), \end{cases} \tag{5}$$

where $\Xi(t) \in \mathcal{D}(A) \subset X$. The relation between corresponding solutions of (5) and (1) is given by $\Xi_0(t) = x(t)$ and $\Xi_1(t)(\theta) \equiv x(t + \theta)$ for $\theta \in [-\tau_m, 0]$.

2.1 Computation of Characteristic Roots and the Spectral Abscissa

The spectral properties of the operator $\mathcal{A}$ in (5) are described in detail in Michiels and Niculescu (2014, Chap. 1). The operator only has a point spectrum. Hence, its spectrum, $\sigma(\mathcal{A})$, is fully determined by the eigenvalue problem

$$\mathcal{A}\, z = \lambda z,\ z \in X,\ z \neq 0. \tag{6}$$

The connections with the characteristic roots are as follows. The characteristic roots are the eigenvalues of operator $\mathcal{A}$. Moreover, if $\lambda \in \sigma(\mathcal{A})$, then the corresponding eigenfunction takes the form

$$z(\theta) = ve^{\lambda\theta}, \theta \in [-\tau_m, 0], \tag{7}$$

where $v \in \mathbb{C}^n$ and the pair (λ, v) satisfies (2). Conversely, if a pair (λ, v) satisfies (2), then (7) is an eigenfunction of $\mathcal{A}$ corresponding to the eigenvalue λ. From the equivalent representation of (1) as (5), we conclude that the characteristic roots can be equivalently expressed as

1. the solutions of the finite-dimensional nonlinear eigenvalue problem (2);
2. the solutions of the infinite-dimensional linear eigenvalue problem (6).

This dual viewpoint lies at the basis of available tools to compute the rightmost characteristic roots. On the one hand, discretizing (6) and solving the resulting standard eigenvalue problems allows to obtain global information, for example, estimates of *all* characteristic roots in a given compact set or in a given right half plane. On the other hand, the (finitely many) nonlinear equations (2) allow us to make *local corrections* on characteristic root approximations up to the desired accuracy, e.g., using Newton's method or inverse residual iteration.

There are several possibilities to discretize eigenvalue problem (6). Given a positive integer N and a mesh Ω_N of $N+1$ distinct points in the interval $[-\tau_m, 0]$,

$$\Omega_N = \{\theta_{N,i},\ i = 1, \ldots, N+1\}, \tag{8}$$

with

$$-\tau_m \leq \theta_{N,1} < \ldots < \theta_{N,N} < \theta_{N,N+1} = 0,$$

a spectral discretization as in Breda et al. (2005) (see also Breda 2023) leads for example to the eigenvalue problem

$$\mathcal{A}_N \mathbf{x}_N = \lambda \mathbf{x}_N, \mathbf{x}_N \in \mathbb{C}^{n(N+1)}, \mathbf{x}_N \neq 0, \tag{9}$$

where

$$\mathcal{A}_N = \begin{bmatrix} d_{1,1} & \ldots & d_{1,N+1} \\ \vdots & & \vdots \\ d_{N,1} & \ldots & d_{N,N+1} \\ a_1 & \ldots & a_{N+1} \end{bmatrix} \in \mathbb{R}^{n(N+1)\times n(N+1)} \tag{10}$$

and

$$\begin{aligned} d_{i,k} &= l'_{N,k}(\theta_{N,i}) I_n, && i = 1, \ldots, N, k = 1, \ldots, N+1, \\ a_k &= A_0 l_{N,k}(0) + \sum_{i=1}^{m} A_i l_{N,k}(-\tau_i), && k = 1, \ldots, N+1. \end{aligned}$$

The functions $l_{N,k}$ represent the Lagrange polynomials relative to the mesh Ω_N, i.e. polynomials of degree N such that, $l_{N,k}(\theta_{N,i}) = 1$ if $i = k$ and $l_{N,k}(\theta_{N,i}) = 0$ if $i \neq k$, In Breda et al. (2005) it is proven that spectral accuracy on the individual characteristic root approximations (approximation error $O(N^{-N})$) is obtained with a mesh consisting of (scaled and shifted) Chebyshev extremal points, that is,

$$\theta_{N,i} = -\cos \frac{\pi(i-1)}{N},\ i = 1, \ldots, N+1.$$

The discretization of (6) into (9) lays at the basis of the software tool TRACE-DDE (Breda et al. 2009). The stability routine for equilibria of the package DDE-BIFTOOL (Engelborghs et al. 2002; Sieber et al. 2016) exploits the dual representation of the

eigenvalue problem, since it is based on discretizing the solution operator of (5), whose infinitesimal generator is $\mathcal{A}$, using a spline collocation approach, followed by Newton corrections on (2). For a pseudospectral collocation approach to discretize the solution operator see Breda (2023).

Both aforementioned tools rely on computing all eigenvalues of the discretized system, which restricts the size of the problem from a computational point of view. In Jarlebring et al. (2010) an iterative method is proposed for computing selected eigenvalues of large-scale systems. This method has an interpretation as Arnoldi's method (see, e.g.,Saad 1992) in a function setting, applied to the inverse of the infinite-dimensional operator $\mathcal{A}$, which is characterized in the following proposition.

Proposition 2.1 *The inverse of $\mathcal{A} : X \to X$ exists if and only if matrix $A_0 + \sum_{i=1}^{m} A_i$ is nonsingular. Moreover, it can be explicitly expressed as*

$$\begin{aligned} \mathcal{D}(\mathcal{A}^{-1}) &= X \\ \left(\mathcal{A}^{-1}\,\phi\right)(\theta) &= \left(C(\phi), \int_0^{\theta} \phi_1(s)\,\mathrm{d}s + C(\phi), \theta \in [-\tau_m, 0)\right), \quad \phi \in \mathcal{D}(\mathcal{A}^{-1}), \end{aligned}$$

where

$$C(\phi) = \left(A_0 + \sum_{i=1}^{m} A_i\right)^{-1} \left[\phi_0 - \sum_{i=1}^{m} A_i \int_0^{-\tau_i} \phi_1(s)\,\mathrm{d}s\right]. \tag{11}$$

We note that all information about the system is concentrated in the integration constant (11). To get some insight in the method of Jarlebring et al. (2010), let us apply first the power method to $\mathcal{A}^{-1}$ for scalar system

$$\dot{x}(t) = -2x(t) + \frac{1}{3}x(t - \log 3),$$

whose smallest characteristic root is equal to -1. Starting with the constant initial function $\phi \equiv 1$, the iterations result in polynomials of increasing degree

$$\begin{aligned} &1. \\ &1. - 1.21993t \\ &1. - 1.03416t + .630804t^2 \\ &1. - .999697t + .516927t^2 - .210204t^3 \\ &1. - .998615t + .499156t^2 - .172070t^3 + 0.0524783t^4 \\ &1. - .999733t + .499174t^2 - .166341t^3 + 0.0430061t^4 - 0.0104929t^5 \\ &1. - 1.00000t + .499869t^2 - .166392t^3 + 0.0415855t^4 - 0.00860127t^5 + 0.00174882t^6, \end{aligned}$$

in which one easily recognizes an approximation of the Taylor series of function $\exp(-t)$, the eigenfunction of $\mathcal{A}$ corresponding to eigenvalue $\lambda = -1$, which is closest to the origin. In order to compute multiple eigenvalue approximations, the power method can be replaced by Arnoldi's method, furnishing the basis of the Infinite Arnoldi method (Jarlebring et al. 2010), or by a Rational Krylov method, laying the basis of the dynamic variants of the algorithm proposed in Güttel et al. (2014). As features of interest, these methods do not explicitly rely on a discretization

of the delay equation, while all operations are still performed on vectors and matrices (of finite dimension), in addition to their ability to exploit sparsity of the coefficient matrices.

We note that also methods for generic nonlinear eigenvalue problems can be used for computing characteristic roots, see for instance the CORK framework described in Van Beeumen et al. (2015) and the software package NEP-PACK (Jarlebring et al. 2018).

2.2 Computation of $\mathcal{H}_\infty$ Norms

For systems without delay, level set methods are standard methods for computing $\mathcal{H}_\infty$ norms and related problems, see, e.g., Boyd and Balakrishnan (1990), Bruinsma and Steinbuch (1990) and the references therein. These methods originate from the property that all the intersections of the singular value curves, corresponding to the transfer function, and a constant function (the level) can be directly computed from the solutions of a structured eigenvalue problem. This property enables a fast two-directional search for the dominant peak in the singular value plot.

In Michiels and Gumussoy (2010) an extension of this approach for computing the $\mathcal{H}_\infty$ norm of transfer function (3) is described. The theoretical foundation is contained in the following proposition from Michiels and Gumussoy (2010, Lemma 2.1 and Proposition 2.2).

Proposition 2.2 *Let $\xi > 0$ be such that the matrix $D_\xi := D^T D - \xi^2 I$ is non-singular. For $\omega \geq 0$, matrix $G(i\omega)$ in (3) has a singular value equal to ξ if and only if $\lambda = i\omega$ is a solution of the equation*

$$\det H(\lambda; \xi) = 0, \tag{12}$$

where

$$H(\lambda; \xi) := \lambda I - M_0 - \sum_{i=1}^{m} \left(M_i e^{-\lambda \tau_i} + M_{-i} e^{\lambda \tau_i} \right) - \left(N_1 e^{-\lambda \tau_0} + N_{-1} e^{\lambda \tau_0} \right),$$

with

$$M_0 := \begin{bmatrix} A_0 & -B D_\xi^{-1} B^T \\ -C^T C + C^T D D_\xi^{-1} D^T C & -A_0^T \end{bmatrix},$$
$$M_i := \begin{bmatrix} A_i & 0 \\ 0 & 0 \end{bmatrix}, \; M_{-i} := \begin{bmatrix} 0 & 0 \\ 0 & -A_i^T \end{bmatrix}, \; 1 \leq i \leq m,$$
$$N_1 := \begin{bmatrix} 0 & 0 \\ 0 & C^T D D_\xi^{-1} B^T \end{bmatrix}, \; N_{-1} := \begin{bmatrix} -B D_\xi^{-1} D^T C & 0 \\ 0 & 0 \end{bmatrix}.$$

Moreover, (12) holds if and only if λ is an eigenvalue of the operator $\mathcal{L}_\xi$, defined by

$$\mathcal{D}(\mathcal{L}_\xi) := \Big\{\phi \in Z : \ \phi'(0) = M_0\phi(0) + \sum_{i=1}^{m} (M_i\phi(-\tau_i) + M_{-i}\phi(\tau_i)) + N_1\phi(-\tau_0) + N_{-1}\phi(\tau_0)\Big\}$$

$$\mathcal{L}_\xi\, \phi := \phi', \quad \phi \in \mathcal{D}(\mathcal{L}_\xi),$$

where $Z := AC([-\tau_m, \tau_m], \mathbb{C}^{2n})$.

According to Proposition 2.2, the intersections of the constant function $\mathbb{R} \ni \omega \mapsto \xi$, with level $\xi > 0$ prescribed, and the curves

$$\mathbb{R} \ni \omega \mapsto \sigma_i(G(\mathrm{i}\omega)), \ 1 \le i \le \min(n_\zeta, n_\eta),$$

where $\sigma_i(\cdot)$ denotes the ith singular value, can be found by computing the solutions on the imaginary axis of either

1. the finite-dimensional nonlinear eigenvalue problem,

$$H(\lambda; \xi)v = 0, v \in \mathbb{C}^{2n}, \ v \neq 0, \ \text{or} \tag{13}$$

2. the infinite-dimensional linear eigenvalue problem

$$\mathcal{L}_\xi\phi = \lambda\phi, \phi \in Z, \phi \neq 0.$$

These two characterizations are similar to the representations of characteristic roots as eigenvalues. As a consequence, the methods outlined in Sect. 2.1 can be adapted accordingly.

The method presented in Michiels and Gumussoy (2010) for computing the $\mathcal{H}_\infty$ norm of (3) relies on a two-directional search in a modification of the singular value plot, induced by a spectral discretization of operator $\mathcal{L}_\xi$, followed by a local correction of the peak value up to the desired accuracy. The latter is based on the nonlinear equation (13), supplemented with a local optimality condition. The main steps are sketched in Fig. 1.

Finally, a closely related problem is the computation of the pseudospectral abscissa, for which we refer to Gumussoy and Michiels (2010) and the references therein.

2.3 Computation of $\mathcal{H}_2$ Norms

We assume that (1) is internally exponentially stable and, in addition, that matrix D is equal to zero. Under these conditions the $\mathcal{H}_2$ norm of G is finite and it satisfies (4). We present two different approaches for its computation, which once again stem

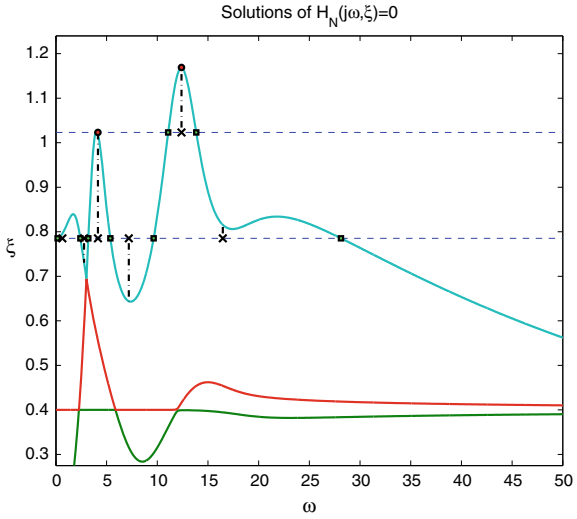

Fig. 1 Principles of the method in Michiels and Gumussoy (2010). Function H_N is an approximation of H, induced by a spectral discretization of $\mathcal{L}_\xi$ on a mesh consisting of $2N+1$ points over the interval $[-\tau_m, \tau_m]$. In the first step the peak value is found for a fixed value of N by the iterative algorithm of Bruinsma and Steinbuch (1990): for a given level ξ all intersections with the approximate singular value curves are computed (squares). In the geometric midpoints of these intersections (crosses) a vertical search for intersections is performed. The maximum value of ξ over all the intersections gives rise to the new value of the level. In the second step, the effect of the discretization is removed by a local corrector based on nonlinear eigenvalue problem (13) (circles)

from the two descriptions of the time-delay system, by the functional differential equation (1) and by the abstract linear equation (5), respectively.

The first approach makes use of so-called delay-Lyapunov equations, introduced in the context of constructing complete-type Lyapunov-Krasovskii functionals for stability assessment (see for instance Kharitonov and Plischke 2006). The following result is a special case of Jarlebring et al. (2011, Theorem 1).

Theorem 1 *Assume that (1) is internally exponentially stable and $D = 0$. Then the $\mathcal{H}_2$ norm of transfer function (3) satisfies*

$$\begin{aligned} \|G\|_{\mathcal{H}_2} &= \mathrm{tr}(B^T U(0) B), \\ &= \mathrm{tr}(C V(0) C^T), \end{aligned}$$

where U, V are the unique solutions of the delay Lyapunov equation

$$\begin{cases} U'(t) = U(t)A_0 + \sum_{k=1}^{m} U(t-\tau_k)A_k, \quad t \in [0, \tau_1], \\ U(-t) = U^T(t), \\ -C^TC = U(0)A_0 + A_0^T U(0) + \sum_{k=1}^{m} \left(U^T(\tau_k)A_k + A_k^T U(\tau_k)\right), \end{cases} \tag{14}$$

and the dual delay Lyapunov equation

$$\begin{cases} V'(t) = V(t)A_0^T + \sum_{k=1}^{m} V(t-\tau_k)A_k^T, \ t \in [0, \tau_{\max}], \\ V(-t) = V^T(t), \\ -BB^T = V(0)A_0^T + A_0V(0) + \sum_{k=1}^{m} \left(V^T(\tau_k)A_k^T + A_kV(\tau_k)\right). \end{cases} \tag{15}$$

The underlying idea in the proof is that the solutions of (14)–(15), as well as the $\mathcal{H}_2$ norm, can be expressed in terms of the *fundamental solution* of the delay equation (see, e.g., Kharitonov and Plischke 2006; Jarlebring et al. 2011).

Theorem 1 opens the possibility to compute $\mathcal{H}_2$ norms by solving delay Lyapunov equations numerically. An approach based on spectral collocation on a Chebyshev mesh is presented in Jarlebring et al. (2011). This approach is generally applicable, but the convergence rate of the approximation (as a function of the number of mesh points) depends on the smoothness properties of the solution, which are on their turn determined by the interdependence of the delays (see Sect. 4 of the reference for a complete characterization). It is also shown that, in the case of commensurate delay values, an analytic solution of (14)–(15) can be obtained, which leads to an *explicit* expression for the $\mathcal{H}_2$ norm involving only matrices of finite dimension.

The second approach is based on discretizing (5). A spectral discretization on the mesh (8) leads us to the linear system

$$\begin{cases} \dot{\mathbf{x}}_N(t) = \mathcal{A}_N\mathbf{x}_N(t) + \mathcal{B}_N\zeta(t), \\ \eta(t) \quad = \mathcal{C}_N\mathbf{x}_N(t), \end{cases} \tag{16}$$

where $\mathcal{A}_N$ is given by (10) and

$$\mathcal{B}_N = [0 \ \cdots \ 0 \ I]^T \otimes B, \mathcal{C}_N = [0 \ \cdots \ 0 \ I] \otimes C.$$

From the fact that (16) is a standard linear time-invariant system we can approximately compute

$$\begin{aligned} \|G\|_{\mathcal{H}_2} \approx \|G_N\|_{\mathcal{H}_2} &= \operatorname{tr}(\mathcal{B}^T Q_N \mathcal{B}_N) \\ &= \operatorname{tr}(\mathcal{C}_N P_N \mathcal{C}^T), \end{aligned}$$

where G_N is the transfer function of (16) and the pair (P_N, Q_N) satisfies (see, e.g., Zhou et al. 1995),

$$\begin{aligned} \mathcal{A}_N P_N + P_N \mathcal{A}_N^T &= -\mathcal{B}_N \mathcal{B}_N^T, \\ \mathcal{A}_N^T Q_N + Q_N \mathcal{A}_N &= -\mathcal{C}_N^T \mathcal{C}_N. \end{aligned} \tag{17}$$

In Vanbiervliet et al. (2011) it has been shown that the approximation error satisfies

$$\|G\|_{\mathcal{H}_2} - \|G_N\|_{\mathcal{H}_2} = \mathcal{O}(N^{-3}), \ N \to \infty,$$

while arguments are provided why fairly accurate results are expected for a moderate value of N already.

Although the second approach is essentially a "discretize first" approach, it is amendable for most control problems because, unlike the delay Lyapunov equation approach of Jarlebring et al. (2011), it does not involve an explicit vectorization of matrix equations (which squares the dimensions of the problem), and because derivatives of the $\mathcal{H}_2$ norm with respect to the elements of the system matrices in (3) can easily be obtained as a by-product of solving (17), see Vanbiervliet et al. (2011).

Finally, for large-scale problems involving sparse coefficient matrices, a discretization-free method has been proposed in Michiels and Zhou (2019), which is related to the infinite Arnoldi method discussed at the end of Sect. 2.1.

3 Making the Leap From Analysis to Synthesis

In what follows we assume that the system matrices in (1) smoothly depend on a finite number of parameters $p = (p_1, \ldots, p_{n_p}) \in \mathbb{R}^{n_p}$. Making the dependence explicit in the notations leads us to system

$$\begin{cases} \dot{x}(t) = A_0(p)x(t) + \sum_{i=1}^{m} A_i(p)x(t-\tau_i) + B(p)\zeta(t), \\ \eta(t) = C(p)x(t) + D(p)\zeta(t-\tau_0). \end{cases} \tag{18}$$

In many control design problems the *closed-loop* system can be brought into the form (18), where the parameters p have an interpretation in terms of a parametrization of the controller, while ζ and η appear as external inputs and outputs, used in the description of performance and robustness specifications. We note that both static and dynamic controllers can be addressed in this framework. It is also possible to impose additional structure on the controller, such as a proportional-integral-derivative (PID) structure, or to impose a sparsity pattern, enabling the design of decentralized and distributed controllers (Dileep et al. 2018).

Because time-delay systems constitute a class of infinite-dimensional systems, illustrated by representation (5) and by the typical presence of infinitely many characteristic roots, *any* control design problem involving the determination of a finite number of parameters can be interpreted as a reduced-order controller synthesis

problem. This explains to a large extent the difficulties and limitations in controlling time-delay systems (Niculescu 2001; Sipahi et al. 2011; Michiels 2019).

The proposed control synthesis methods are based on a direct optimization of appropriately defined cost functions as a function of the parameters p.

3.1 Stabilization

In order to impose internal exponential stability of the null solution of (18), it is necessary to find values of p for which the spectral abscissa

$$c(p) := \sup_{\lambda \in \mathbb{C}} \left\{ \Re(\lambda) : \det \left(\lambda I - A_0(p) - \sum_{i=1}^{m} A_i(p) e^{-\lambda \tau_i} \right) = 0 \right\}$$

is strictly negative. The approach of Vanbiervliet et al. (2008) is based on minimizing the function

$$p \to c(p). \tag{19}$$

Function (19) is in general non convex. It may be not everywhere differentiable, even not everywhere Lipschitz continuous. A lack of differentiability may occur when there are more than one *active* characteristic roots, i.e., a characteristic roots whose real part equals the spectral abscissa. A lack of Lipschitz continuity may occur when an active characteristic roots is multiple and non-semisimple. On the contrary, the spectral abscissa function is differentiable at points where there is only one active characteristic root with multiplicity one. If this is the case with probability one when randomly sampling parameter values, the spectral abscissa is smooth almost everywhere (Vanbiervliet et al. 2008).

The properties of function (19) preclude the use of standard optimization methods, developed for smooth problems. Instead we propose the Broyden-Fletcher-Goldfarb-Shanno (BFGS) algorithm with weak Wolfe line search, whose favorable properties for nonsmooth problems have been reported in Lewis and Overton (2009), with refinements using the gradient sampling algorithm (Burke et al. 2005). This combination of algorithms has been implemented in the MATLAB code HANSO (Overton 2009). The code only requires the evaluation of the objective function, as well as its derivatives with respect to parameters, *whenever* it is differentiable.

The value of the spectral abscissa can be obtained by computing the rightmost characteristic roots, using the methods described in Sect. 2.1. If there is only one active characteristic root λ_a with multiplicity one, the spectral abscissa is differentiable and we can express

$$\frac{\partial c}{\partial p_k}(p) = \Re \left(\frac{w^H \left(\frac{\partial A_0}{\partial p_k}(p) + \sum_{i=1}^{m} \frac{\partial A_i}{\partial p_k}(p) e^{-\lambda_a \tau_i} \right) v}{w^H \left(I + \sum_{i=1}^{m} A_i(p) \tau_i e^{-\lambda_a \tau_i} \right) v} \right)$$

for $k = 1, \ldots, n_p,$, where w and v are the left and right eigenvector corresponding to eigenvalue λ_a.

3.2 Optimizing $\mathcal{H}_\infty$ and $\mathcal{H}_2$ Norms

The properties of the function

$$p \mapsto \|G(\cdot;\, p)\|_{\mathcal{H}_\infty}, \tag{20}$$

where $G(\lambda;\, p)$ is the transfer function of (18), are very similar to the spectral abscissa function. In particular, function (20) is in general not convex, not everywhere differentiable, but it is smooth almost everywhere. Consequently, the methods described in Sect. 3.1 can also be applied to (20). For almost all p derivatives exist and they can be computed from the sensitivity of an individual singular value of $G(\mathrm{i}\omega;\, p)$ with respect to p, for a fixed value of ω, see Gumussoy and Michiels (2011). Unlike objective function (20), function

$$p \mapsto \|G(\cdot;\, p)\|_{\mathcal{H}_2}, \tag{21}$$

is smooth whenever it is finite, which allows an embedding in a derivative based optimization framework. Derivatives of (21) can be obtained either by constructing the *variational equation* corresponding to (14), as worked out in Gomez et al. (2019), or, in a discretize-first setting, from the solutions of the two Lyapunov matrix equations in (17), see Vanbiervliet et al. (2011).

The minimization problems of (20) and (21) contain an implicit constraint, $c(p) < 0$, because the norms are only finite if the system is internally exponentially stable. This leads us to a two-stage approach: if the initial values of the parameters are not stabilizing, then the overall procedure contains a preliminary stabilization phase, using the methods of Sect. 3.1. For the next phase, the actual minimization of (20)–(21), the line-search mechanism in BFGS and the gradient sampling algorithm are adapted in order to discard trial steps or samples outside the feasible set, defined by the implicit constraint (Gumussoy and Michiels 2011).

Instead of directly optimizing the spectral abscissa as in Sect. 3.1, which requires methods for nonsmooth optimization problems, it is also possible to optimize a smooth relaxation of the spectral abscissa function, proposed in Vanbiervliet et al. (2009b), Gomez and Michiels (2019b), which is defined in terms of a relaxed $\mathcal{H}_2$ criterion. In this way stability optimization can also be performed within a derivative based framework. Moreover, an adaptation of the approach makes it possible to solve $\mathcal{H}_2$ optimization problems without the explicit need for a preliminary stabilization phase (Vanbiervliet et al. 2009a).

4 Case Studies

In this section we illustrate the flexibility of the presented control design approach. With the first example from Michiels et al. (2010), we show how to incorporate pole location constraints in the stabilization procedure. The additional flexibility consists of assigning a finite number of characteristic roots, smaller or equal than the number of controller parameters, and using the remaining degrees of freedom to optimize the real part of the rightmost non-assigned characteristic root. With the second example from Gomez et al. (2019), we illustrate the design of a proportional-retarded controller, thereby optimizing a cost function expressed in terms of the $\mathcal{H}_2$ norm and using a delay as a controller parameter.

Example 4.1 Many design criteria for linear control systems, such as the settling time, damping and amount of overshoot, can be translated into a desired location of the rightmost characteristic roots. The characteristic matrix of (18) is given by

$$\Delta(\lambda;\, p) := \lambda I - A_0(p) - \sum_{i=1}^{m} A_i(p) e^{-\lambda \tau_i}.$$

Assigning a real characteristic root to the location r results into the following constraint on the parameter values,

$$\det\left(\Delta(r;\, p)\right) = 0. \tag{22}$$

Similarly, assigning a complex conjugate pair of characteristic roots, $r \pm sj$, results in the constraints

$$\Re\left(\det\left(\Delta(r \pm sj;\, p)\right)\right) = 0;\ \ \Im\left(\det\left(\Delta(r \pm sj;\, p)\right)\right) = 0. \tag{23}$$

If matrix Δ depends in an affine way on p and if the condition

$$\operatorname{rank}\left(\left[\frac{\partial \Delta}{\partial p_1}(\lambda;\, p)\ \cdots\ \frac{\partial \Delta}{\partial p_{n_p}}(\lambda;\, p)\right]\right) = 1,\ \ \forall \lambda \in \mathbb{C}, \tag{24}$$

is satisfied, then the constraints (22)–(23) are affine in p. Hence, assigning k characteristic roots, with $k \leq n_p$, can be expressed by constraints of the form

$$Sp = R, \tag{25}$$

where $S \in \mathbb{R}^{k \times n_p}$ and $R \in \mathbb{R}^{k \times 1}$. It is important to note that the rank condition (24) is satisfied for problems where the closed-loop characteristic matrix results from control through a single input.

In article Michiels et al. (2010) it is shown how the constraints (25) on the parameters can be eliminated. Subsequently, the optimization problem

$$\min_{p\in\mathbb{R}^{n_p},\ Sp=R} \bar{c}(p) \tag{26}$$

is addressed, where

$$\bar{c}(p) := \sup_{\lambda\in\mathbb{C}} \left\{ \Re(\lambda) : \frac{\det\left(\lambda I - A_0(p) - \sum_{i=1}^{m} A_i(p)e^{-\lambda\tau_i}\right)}{\Pi_{i=1}^{k}(\lambda-\lambda_i)} = 0 \right\} \tag{27}$$

and $\{\lambda_1, \ldots, \lambda_k\}$ are the assigned characteristic roots. Problem (26) is a modification of the spectral abscissa minimization problem discussed in Sect. 3.1. Since the assigned roots are specified by the designer, the value of (27) can be obtained by computing the rightmost characteristic roots and removing the assigned ones, which are invariant over the (reduced) controller parameter space.

Let us now consider the solution of problem (26) for the model of an experimental heat transfer set-up at the Czech Technical University in Prague, comprehensively described in Vyhlídal et al. (2009). The model consists of 10 delay differential equations. The addition of an integrator, to achieve a zero steady state error of one of the controlled state variables with respect to a prescribed set-point, eventually results in equations of the form

$$\dot{x}(t) = A_0 x(t) + \sum_{i=1}^{5} A_i x(t-\tau_i) + Bu(t-\tau_6), \tag{28}$$

with $x(t) \in \mathbb{R}^{11\times 11}$ and $u(t) \in \mathbb{R}$. We refer to Vyhlídal et al. (2009) for the corresponding matrices and delay values. In Fig. 2 we show the rightmost characteristic roots of the open-loop system. For the control law

$$u(t) = \sum_{i=1}^{11} p_i x_i(t),$$

the solutions of optimization problem (26) are presented in Table 1. The setting SN1 corresponds to the (unconstrained) minimization of the spectral abscissa (19). The other settings correspond to assigning one real characteristic root (SN2), one pair of complex conjugate characteristic roots (SN3) and, finally, two real roots and two complex conjugate roots (SN4). The assigned characteristic roots were chosen to the right of the minimum of the spectral abscissa function, because these root were intended to become the rightmost roots after solving (26). Their positions were optimized to achieve a properly damped set-point response and disturbance rejection (Michiels et al. 2010). The optimized characteristic root locations are shown in Fig. 3 for settings SN1 and SN4.

Example 4.2 We consider a second-order, oscillatory system of the form

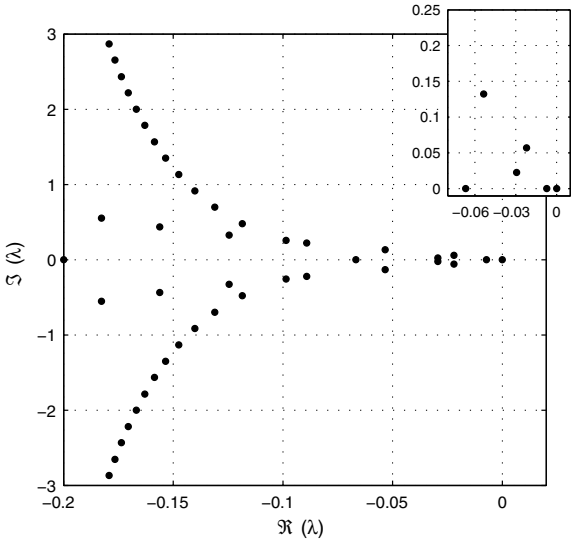

Fig. 2 Rightmost characteristic roots of the open-loop system (28)

Table 1 Controller parameters corresponding to the solution of (26), see the main text for more details

SN	1	2	3	4
λ_i	- - - -	-0.01	$-0.02 \pm 0.02i$	$-0.02, -0.03$ $-0.03 \pm 0.03i$
$\min \bar{c}$	-0.0565	-0.0629	-0.0659	-0.0736
p_1	-5.4349	-0.0732	-4.1420	-0.3521
p_2	3.5879	8.1865	5.9345	8.6190
p_3	-1.4411	-1.2503	-2.3820	-4.8822
p_4	-3.7043	-7.1472	-7.9449	-17.2747
p_5	24.616	32.8003	27.8585	35.1494
p_6	-2.1778	4.4977	0.4490	-1.3188
p_7	9.6924	10.3140	8.4887	6.0338
p_8	-4.5121	-2.6572	-0.2605	5.4190
p_9	-14.631	-21.6711	-20.5152	-24.6596
p_{10}	11.351	4.1244	5.4531	2.3754
p_{11}	-0.7562	-0.2749	-0.3635	-0.1360

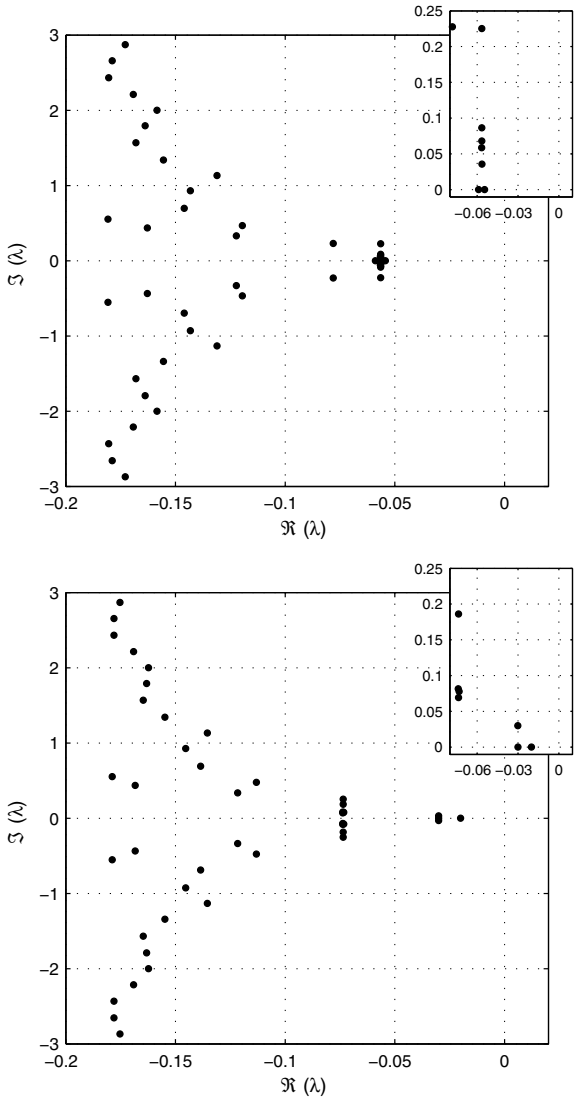

Fig. 3 Rightmost characteristic roots corresponding to the solution of (26), for settings SN1 and SN4 in Table 1

$$\begin{aligned} \dot{x}(t) &= Ax(t) + B(u(t) + \zeta(t)) \\ y(t) &= Cx(t), \\ \eta(t) &= Cx(t), \end{aligned} \tag{29}$$

with matrices

$$A = \begin{bmatrix} 0 & 1 \\ -\nu^2 & -2\delta\nu \end{bmatrix}, \; B = \begin{bmatrix} 0 \\ b \end{bmatrix}, \; C = \begin{bmatrix} 1 & 0 \end{bmatrix},$$

where ν is the natural frequency, δ is the damping factor, and b is the input gain. We introduce a Proportional-Retarded (PR) controller of the form

$$u(t) = -k_p y(t) + k_r y(t - \tau_1), \tag{30}$$

where we consider k_r and τ_1 as parameters. This class of controllers, where the delay is a design parameter, has been studied in recent works (see, for instance, Villafuerte et al. 2013). As a main motivation from an application perspective, controller (30) mimics the behavior of a proportional-derivative (PD) controller, without the need to explicitly differentiate the output, which might amplify sensor noise considerably. The closed-loop system, formed by coupling (29) with (30), is given by

$$\begin{aligned} \dot{x}(t) =& \begin{bmatrix} 0 & 1 \\ -\nu^2 - bk_p & -2\delta\nu \end{bmatrix} x(t) + \begin{bmatrix} 0 & 0 \\ bk_r & 0 \end{bmatrix} x(t - \tau_1) + \begin{bmatrix} 0 \\ b \end{bmatrix} \zeta(t) \\ \eta(t) =& Cx(t). \end{aligned} \tag{31}$$

In order to bring this system model in the form of (18), we perform a transformation of time. Setting $\bar{x}(\bar{t}) = x(t)$, with $t = \tau_1 \bar{t}$, we arrive at

$$\begin{aligned} \dot{\bar{x}}(\bar{t}) =& \begin{bmatrix} 0 & \tau_1 \\ -\nu^2\tau_1 - bk_p\tau_1 & -2\delta\nu\tau_1 \end{bmatrix} \bar{x}(\bar{t}) + \begin{bmatrix} 0 & 0 \\ bk_r\tau_1 & 0 \end{bmatrix} \bar{x}(\bar{t} - 1) \\ &+ \begin{bmatrix} 0 \\ b\tau_1 \end{bmatrix} \zeta(\tau_1 \bar{t}) \\ \eta(\tau_1 \bar{t}) =& C\bar{x}(\bar{t}). \end{aligned} \tag{32}$$

The relation between the $\mathcal{H}_2$ norm of systems (31) and (32) is given as follows:

$$\|G\|_{\mathcal{H}_2}^2 = \frac{1}{\tau_1} \|\bar{G}\|_{\mathcal{H}_2}^2, \tag{33}$$

where $\bar{G}$ is the transfer function of the time-scaled system (32). We use this equality in order to minimize $\|G\|_{\mathcal{H}_2}^2$. We set the following numerical values, corresponding to the model of a DC servomechanism in Villafuerte et al. (2013),

$$\nu = 17.6,\ \delta = 0.0128,\ b = 31,\ k_p = 22.57,$$

and take as parameter vector $p = [p_1\ p_2]$, with $p_1 = \tau_1$ and $p_2 = k_r\tau_1$. From (33), the gradient of $\|G\|_{\mathcal{H}_2}^2$ with respect to p can be expressed as

$$\nabla \|G\|_{\mathcal{H}_2}^2 = \frac{1}{p_1} \begin{bmatrix} \dfrac{\partial \|\bar{G}\|_{\mathcal{H}_2}^2}{\partial p_1} - \dfrac{\|\bar{G}\|_{\mathcal{H}_2}^2}{p_1} \\ \dfrac{\partial \|\bar{G}\|_{\mathcal{H}_2}^2}{\partial p_2} \end{bmatrix}.$$

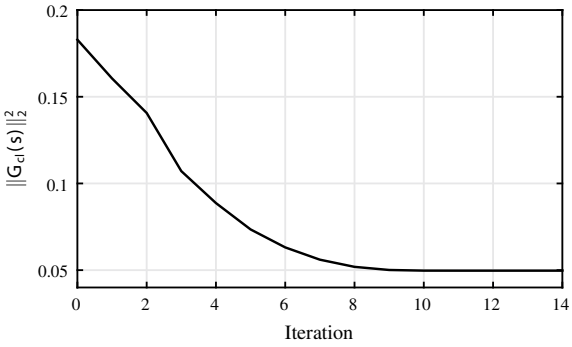

Fig. 4 Values of $\|G\|_{\mathcal{H}_2}^2$ at every iteration, corresponding to Example 4.2

The values of the delay and the gain obtained by minimization of the $\mathcal{H}_2$ norm of system (31), with initial parameters $p = [0.03\ 0.09]$, are given by $\tau_1 = 0.05187$ and $k_r = 17.9643$, while the achieved value of $\|G\|_{\mathcal{H}_2}^2$ is 0.0497. Figure 4 shows the value of the $\mathcal{H}_2$ norm of system (31) at every iteration of the optimization of function (33).

5 Equations of Neutral Type and Delay Differential Algebraic Equations

In this section we consider delay differential algebraic equation (DDAE) models of the form

$$\begin{cases} E\dot{x}(t) = A_0 x(t) + \sum_{i=1}^{m} A_i x(t-\tau_i) + B\zeta(t), \\ \eta(t) = Cx(t), \end{cases} \tag{34}$$

where leading matrix E is singular, $x(t) \in \mathbb{C}^n, \zeta(t) \in \mathbb{C}^{n_\zeta}$, $\eta(t) \in \mathbb{C}^{n_\eta}$ are the (pseudo)state, input and output at time t, and $0 < \tau < \cdots < \tau_m$ represent the time-delays. With the following examples we illustrate the generality of model (34).

Example 5.1 Consider the feedback interconnection of system

$$\begin{cases} \dot{x}(t) = Ax(t) + B_1 u(t) + B_2 \zeta(t), \\ y(t) = Cx(t) + D_1 u(t), \\ \eta(t) = Fx(t), \end{cases}$$

and controller

$$u(t) = Ky(t-\tau).$$

For $\tau = 0$, it is possible to eliminate the output and the controller equation, which results in the closed-loop system

$$\begin{cases} \dot{x}(t) = Ax(t) + B_1K(I - D_1K)^{-1}Cx(t) + B_2\zeta(t), \\ \eta(t) = Fx(t). \end{cases} \tag{35}$$

This approach is for instance taken in the software package HIFOO (Burke et al. 2006). If $\tau \neq 0$, then the elimination is not possible any more. However, if we let $X = [x^T\ u^T\ y^T]^T$ we can describe the system by the equations

$$\begin{cases} \begin{bmatrix} I & 0 & 0 \\ 0 & 0 & 0 \\ 0 & 0 & 0 \end{bmatrix} \dot{X}(t) = \begin{bmatrix} A & B_1 & 0 \\ C & D_1 & -I \\ 0 & I & 0 \end{bmatrix} X(t) - \begin{bmatrix} 0 & 0 & 0 \\ 0 & 0 & 0 \\ 0 & 0 & K \end{bmatrix} X(t-\tau) + \begin{bmatrix} B_2 \\ 0 \\ 0 \end{bmatrix} \zeta(t), \\ \eta(t) = \begin{bmatrix} F & 0 & 0 \end{bmatrix} X(t), \end{cases}$$

which are of the form (34). Furthermore, the dependence of the matrices of the closed-loop system on the controller gain K is still linear, unlike in (35).

Example 5.2 The presence of a direct feedthrough term from ζ to η, as in

$$\begin{cases} \dot{x}(t) = A_0x(t) + A_1x(t-\tau) + B\zeta(t), \\ \eta(t) = Fx(t) + D_2\zeta(t), \end{cases} \tag{36}$$

can be avoided by introducing a slack variable. If we let $X = [x^T\ \gamma^T]^T$, where γ is the slack variable, we can bring (36) in the form (34):

$$\begin{cases} \begin{bmatrix} I & 0 \\ 0 & 0 \end{bmatrix} \dot{X}(t) = \begin{bmatrix} A_0 & 0 \\ 0 & -I \end{bmatrix} X(t) + \begin{bmatrix} A_1 & 0 \\ 0 & 0 \end{bmatrix} X(t-\tau) + \begin{bmatrix} B \\ I \end{bmatrix} \zeta(t), \\ \eta(t) = [F\ D_2]\, X(t). \end{cases}$$

In a similar fashion the feedthrough term $Du(t - \tau_0)$ in (1) can be eliminated.

Example 5.3 The following system with input delay and input dynamics,

$$\begin{cases} \dot{x}(t) = Ax(t) + B_1\zeta(t) + B_2\zeta(t-\tau), \\ \eta(t) = Cx(t), \end{cases}$$

can also be brought into standard form (34), again by using a slack variable. Setting $X = [x^T\ \gamma^T]^T$, with (pseudo)state variable γ representing a copy of the input, we can express

$$\begin{cases} \dot{X}(t) = \begin{bmatrix} A & B_1 \\ 0 & -I \end{bmatrix} X(t) + \begin{bmatrix} 0 & B_2 \\ 0 & 0 \end{bmatrix} X(t-\tau) + \begin{bmatrix} 0 \\ I \end{bmatrix} \zeta(t), \\ \eta(t) = [C\ \ 0]\, X(t). \end{cases}$$

In a similar way we can handle multiple delays in the output.

Example 5.4 Neutral type systems can be considered as well. The following neutral equation

$$\frac{\mathrm{d}}{\mathrm{d}t}\left(x(t)+\sum_{i=1}^{m} G_i x(t-\tau_i)\right)=\sum_{i=0}^{m} H_i x(t-\tau_i)$$

can for instance be rewritten as

$$\begin{cases} \dot{\gamma}(t) = \displaystyle\sum_{i=0}^{m} H_i x(t-\tau_i), \\ 0 \;\; = -\gamma(t)+x(t)+\displaystyle\sum_{i=1}^{m} G_i x(t-\tau_i). \end{cases} \tag{37}$$

Clearly (37) is of the form (34), with (pseudo)state $[\gamma(t)^T \; x(t)^T]^T$.

It should be noted that DDAE models are particularly suitable for the (automated) modeling and description of interconnected systems, where the differential equations stem from a systematic description of the subsystems or components, while the algebraic and delay difference equations model their interconnections. As a final illustration, the feedback interconnection of any retarded type time-delay system and controller with the following state-space representations,

$$\begin{cases} \dot{x}_G(t) = \displaystyle\sum_{i=0}^{m_a} A^i x_G(t-\tau_i^a) + \sum_{i=0}^{m_{b_1}} B_1^i \zeta(t-\tau_i^{b_1}) + \sum_{i=0}^{m_{b_2}} B_2^i u(t-\tau_i^{b_2}) \\ \eta(t) = \displaystyle\sum_{i=0}^{m_{c_1}} C_1^i x_G(t-\tau_i^{c_1}) + \sum_{i=0}^{m_{d_{11}}} D_{11}^i \zeta(t-\tau_i^{d_{11}}) + \sum_{i=0}^{m_{d_{12}}} D_{12}^i u(t-\tau_i^{d_{12}}) \\ y(t) = \displaystyle\sum_{i=0}^{m_{c_2}} C_2^i x_G(t-\tau_i^{c_2}) + \sum_{i=0}^{m_{d_{21}}} D_{21}^i \zeta(t-\tau_i^{d_{21}}) + \sum_{i=0}^{m_{d_{22}}} D_{22}^i u(t-\tau_i^{d_{22}}) \end{cases} \tag{38}$$

and

$$\begin{cases} \dot{x}_K(t) = \displaystyle\sum_{i=0}^{m_{a_k}} A_K^i x_K(t-\tau_i^{a_k}) + \sum_{i=0}^{m_{b_k}} B_K^i y(t-\tau_i^{b_k}) \\ u(t) = \displaystyle\sum_{i=0}^{m_{c_k}} C_K^i x_K(t-\tau_i^{c_k}) + \sum_{i=0}^{m_{d_k}} D_K^i u(t-\tau_i^{d_k}), \end{cases} \tag{39}$$

can be written in the form of (34) by combining the techniques illustrated with the previous examples. More precisely, the transformation consists of the elimination of input dynamics, output dynamics, and non-trivial feedthrough terms.

The price to pay for the generality of model (34) is the increase of the dimension of the system, n, compared to classical DDE models, which may affect the efficiency of the numerical methods. However, this is a minor problem in most of the applications, because the delay difference equations or algebraic constraints are related to inputs and outputs, and for large-scale problems the number of inputs and outputs are usually much smaller than the number of state variables. Another consequence of the generality is that assumptions for well-posedness are necessary (in the next

subsection we will introduce such an assumption). To illustrate the necessity, the DDAE

$$\begin{aligned} \dot{x}_1(t) &= x_1(t) + x_2(t-\tau_1) \\ 0 &= -x_2(t-\tau_2) + x_1(t-\tau_3) \end{aligned}$$

is not causal if $\tau_2 > \tau_1 + \tau_3$, following from the underlying delay differential equation $\dot{x}_1(t) = x_1(t) + x_1(t-\tau_1-\tau_3+\tau_2)$.

5.1 Preliminaries and Assumptions

Let matrix E in (34) satisfy

$$\operatorname{rank}(E) = n - \nu,$$

with $1 \leq \nu < n$, and let the columns of matrix $U \in \mathbb{R}^{n\times\nu}$, respectively $V \in \mathbb{R}^{n\times\nu}$, be a (minimal) basis for the right, respectively left nullspace of E, which implies

$$U^T E = 0, \;\; EV = 0.$$

Furthermore we define $U^\perp$ and $V^\perp$ as $n \times (n-\nu)$ matrices whose columns span the orthogonal complement of the column spaces of U and V. Throughout the remainder of the chapter we make the following assumption.

Assumption 5.5 Matrix $U^T A_0 V$ is nonsingular.

Assumption 5.5 implies that the differentiation index of (34) is one, corresponding to a system of semi-explicit DDAEs. It is satisfied for all the examples discussed before. The equations (34) can now be explicitly separated into coupled delay differential and delay difference equations. The pre-multiplication of (34) with matrix

$$\begin{bmatrix} U^{\perp T} \\ -(U^T A_0 V)^{-1} U^T \end{bmatrix}$$

and the substitution

$$x = \begin{bmatrix} V^\perp & V \end{bmatrix} \begin{bmatrix} x_1 \\ x_2 \end{bmatrix},$$

with $x_1(t) \in \mathbb{R}^{n-\nu}$ and $x_2(t) \in \mathbb{R}^\nu$, result in the coupled equations

$$\left\{ \begin{aligned} E^{(11)}\dot{x}_1(t) &= \sum_{i=0}^{m} A_i^{(11)} x_1(t-\tau_i) + \sum_{i=0}^{m} A_i^{(12)} x_2(t-\tau_i) + B_1\zeta(t), \\ x_2(t) &= \sum_{i=0}^{m} A_i^{(21)} x_1(t-\tau_i) + \sum_{i=1}^{m} A_i^{(22)} x_2(t-\tau_i) + B_2\zeta(t), \\ \eta(t) &= C_1 x_1(t) + C_2 x_2(t), \end{aligned} \right. \tag{40}$$

where we have $\tau_0 = 0$,

$$E^{(11)} = U^{\perp T} E V^{\perp},\ A_i^{(11)} = U^{\perp T} A_i V^{\perp},\ A_i^{(12)} = U^{\perp T} A_i V,$$

$$\begin{aligned} A_i^{(21)} &= -(U^T A_0 V)^{-1} U^T A_i V^{\perp},\ i = 0, \ldots, m, \\ A_i^{(22)} &= -(U^T A_0 V)^{-1} U^T A_i V, \quad i = 1, \ldots, m, \end{aligned}$$

and

$$B_1 = U^{\perp T} B,\ B_2 = -(U^T A_0 V)^{-1} U^T B,\ C_1 = C V^{\perp},\ C_2 = C V.$$

In (40) matrix $E^{(11)}$ is invertible, following from

$$\operatorname{rank}(E^{(11)}) = \operatorname{rank}\left(\left[U^{\perp}\ U\right]^T E \left[V^{\perp}\ V\right]\right) = \operatorname{rank}(E) = n - \nu.$$

We consider initial functions φ for Eq. (34) that belong to the set $AC\left([-\tau_m, 0], \mathbb{C}^n\right)$ and call them consistent if the corresponding initial value problem at $t = 0$ has at least one solution (Du et al. 2013). A function $x(t; \varphi)$ is called a (classical) solution if it is absolutely continuous, it satisfies (34) almost everywhere on $[0, \infty)$, and $x(\theta; \varphi) = \varphi(\theta)$ for $\theta \in [-\tau_m, 0]$, where φ is a consistent initial function. For a continuously differentiable input function, the space of consistent initial functions for (34) is given by

$$\mathcal{X} := \left\{ \begin{array}{l} \varphi \in AC\left([-\tau_m, 0], \mathbb{C}^n\right) : \\ \qquad U^T A_0 \varphi(0) + \displaystyle\sum_{i=1}^{m} U^T A_i \varphi(-\tau_i) + U^T B \zeta(0) = 0 \end{array} \right\},$$

which corresponds to the set of initial conditions for which the second equation in (40) is satisfied at $t = 0$. Moreover, for every initial function belonging to $\mathcal{X}$, a forward solution is uniquely defined (Ha and Mehrmann 2012; Du et al. 2013; Fridman 2002). We say that system (34), with zero input, is (internally) exponentially stable if there exist constants $\gamma > 0$ and $\sigma > 0$ such that for every initial condition $\varphi \in \mathcal{X}$, the emanating solution satisfies

$$\|x(t; \varphi)\|_2 \leq \gamma e^{-\sigma t} \left(\sup_{\theta \in [-\tau_m, 0]} \|\varphi(\theta)\|_2 \right),\ \forall t \geq 0.$$

5.2 *Spectral Properties and Stability*

We summarize the main theoretical results from Michiels (2011), addressing the stability of the null solution of (34) for $\zeta \equiv 0$.

Exponential Stability. Stability conditions can still be expressed in terms of the position of the characteristic roots, satisfying

$$\det \Delta(\lambda) = 0,$$

where $\Delta : \mathbb{C} \to \mathbb{C}^{n\times n}$ is the characteristic matrix,

$$\Delta(\lambda) := \lambda E - A_0 - \sum_{i=1}^{m} A_i e^{-\lambda\tau_i}.$$

In particular, we have the following result.

Proposition 5.6 *The null solution of (34) is internally exponentially stable if and only if $c < 0$, where c is the* spectral abscissa*:*

$$c := \sup\{\Re(\lambda) : \det \Delta(\lambda) = 0\}.$$

Continuity of the Spectral Abscissa and Strong Stability. We discuss the dependence of the spectral abscissa of (34) on the delay parameters $\vec{\tau} := (\tau_1, \ldots, \tau_m)$. In general the function

$$\vec{\tau} \in (\mathbb{R}_0^+)^m \mapsto c(\vec{\tau}) \tag{41}$$

is not everywhere continuous, as we shall illustrate with an example later on. In fact the lack of continuity carries over from the spectral properties of delay difference equations (see, e.g., Avellar and Hale 1980; Michiels et al. 2002, 2009). Therefore, we first outline properties of the function

$$\vec{\tau} \in (\mathbb{R}_0^+)^m \mapsto c_D(\vec{\tau}) := \sup\{\Re(\lambda) : \det \Delta_D(\lambda; \vec{\tau}) = 0\}, \tag{42}$$

with

$$\Delta_D(\lambda; \vec{\tau}) := -I + \sum_{i=1}^{m} A_i^{(22)} e^{-\lambda\tau_i}. \tag{43}$$

Note that (43) can be interpreted as the characteristic matrix of the delay difference equation

$$x_2(t) = \sum_{i=1}^{m} A_i^{(22)} x_2(t - \tau_i), \tag{44}$$

which is associated with the neutral equation.

The property that function (42) may not be continuous led in Michiels and Vyhlídal (2005) to the smallest upper bound, which is '*insensitive*' to small delay changes. Letting

$$\mathcal{B}(\vec{\tau}, \epsilon) := \{\vec{\theta} \in (\mathbb{R}^+)^m : \|\vec{\theta} - \vec{\tau}\|_2 < \epsilon\}, \tag{45}$$

we can define the robust spectral abscissa c_D of the delay difference equation (44) as follows.

Definition 5.7 For $\vec{\tau} \in (\mathbb{R}_0^+)^m$, let $C_D(\vec{\tau}) \in \mathbb{R}$ be defined as

$$C_D(\vec{\tau}) := \lim_{\epsilon \to 0+} c_D^{\epsilon}(\vec{\tau}),$$

where

$$c_D^{\epsilon}(\vec{\tau}) := \sup \{c_D(\vec{\tau}_\epsilon) : \vec{\tau}_\epsilon \in \mathcal{B}(\vec{\tau}, \epsilon)\}.$$

Several properties of this upper bound on c_D are listed below (see (Michiels 2011, Sect. 3) for an overview).

Proposition 5.8 *The following assertions hold:*

1. *function*
$$\vec{\tau} \in (\mathbb{R}_0^+)^m \mapsto C_D(\vec{\tau})$$
is continuous;
2. *for every $\vec{\tau} \in (\mathbb{R}_0^+)^m$, the quantity $C_D(\vec{\tau})$ is equal to the unique zero of the strictly decreasing function*
$$\chi \in \mathbb{R} \to f(\chi; \vec{\tau}) - 1,$$
where $f : \mathbb{R} \to \mathbb{R}^+$ is defined by
$$f(\chi; \vec{\tau}) := \max_{\vec{\theta} \in [0,\ 2\pi]^m} \rho \left(\sum_{k=1}^{m} A_k^{(22)} e^{-\chi \tau_k} e^{i\theta_k} \right) \tag{46}$$
and $\rho(\cdot)$ denotes the spectral radius;
3. *$C_D(\vec{\tau}) = c_D(\vec{\tau})$ for rationally independent delays*[2]
4. *for all $\vec{\tau}_1, \vec{\tau}_2 \in (\mathbb{R}_0^+)^m$, we have*
$$\text{sign}\,(C_D(\vec{\tau}_1)) = \text{sign}\,(C_D(\vec{\tau}_2)) =: \Sigma;$$
5. *condition $\Sigma < 0$ (> 0) holds if and only if $\gamma_0 < 1$ (> 1) holds, where*
$$\gamma_0 := \max_{\vec{\theta} \in [0,\ 2\pi]^m} \rho \left(\sum_{k=1}^{m} A_k^{(22)} e^{i\theta_k} \right). \tag{47}$$

We now come back to DDAE (34) and, in particular, the properties of its spectral abscissa function (41). The following two technical lemmas establish connections between the characteristic roots of (34) and the zeros of (43).

[2] The m components of $\vec{\tau} = (\tau_1, \ldots, \tau_m)$ are rationally independent if and only if $\sum_{k=1}^{m} n_k \tau_k = 0,\ n_k \in \mathbb{Z}$ implies $n_k = 0, \forall k = 1, \ldots, m$.

Lemma 5.9 *If c_D is finite, then there exists a sequence $\{\lambda_k\}_{k\geq 1}$ of characteristic roots of (34) satisfying*

$$\lim_{k\to\infty} \Re(\lambda_k) = c_D, \ \lim_{k\to\infty} \Im(\lambda_k) = +\infty.$$

Lemma 5.10 *For every $\epsilon > 0$ the number of characteristic roots of (34) in the half plane*

$$\{\lambda \in \mathbb{C} : \Re(\lambda) \geq C_D(\vec{\tau}) + \epsilon\}$$

is finite.

The lack of continuity of the spectral abscissa function (41) leads us again to an upper bound that takes into account the effect of small delay perturbations.

Definition 5.11 For $\vec{\tau} \in (\mathbb{R}_0^+)^m$, let the *robust spectral abscissa* $C(\vec{\tau})$ of (34) be defined as

$$C(\vec{\tau}) := \lim_{\epsilon\to 0+} c^\epsilon(\vec{\tau}), \tag{48}$$

where

$$c^\epsilon(\vec{\tau}) := \sup\{c(\vec{\tau}_\epsilon) : \vec{\tau}_\epsilon \in \mathcal{B}(\vec{\tau}, \epsilon)\}.$$

The following characterization of the robust spectral abscissa (48) constitutes the main theoretical result of this section.

Proposition 5.12 *The following assertions hold:*

1. *the function*
$$\vec{\tau} \in (\mathbb{R}_0^+)^m \mapsto C(\vec{\tau})$$
is continuous;
2. *for every $\vec{\tau} \in (\mathbb{R}_0^+)^m$, we have*
$$C(\vec{\tau}) = \max(C_D(\vec{\tau}), c(\vec{\tau})).$$

In line with the sensitivity of the spectral abscissa with respect to infinitesimal delay perturbations, which has been resolved by considering the robust spectral abscissa (48) instead, we define the notion of strong stability.[3]

Definition 5.13 The null solution of (34), with zero input, is strongly stable if there exists a number $\hat{\tau} > 0$ such that the null solution of

$$E\dot{x}(t) = A_0 + \sum_{k=1}^{m} A_k x(t - (\tau_k + \delta\tau_k))$$

[3] This terminology is borrowed from the theory of neutral delay differential equations (Hale and Verduyn Lunel 2002; Michiels and Vyhlídal 2005).

is exponentially stable for all $\delta\vec{\tau} \in (\mathbb{R}^+)^m$ satisfying $\|\delta\vec{\tau}\|_2 < \hat{\tau}$ and $\tau_k + \delta\tau_k \geq 0,\ k = 1, \ldots, m$.

The following result provides necessary and sufficient conditions for strong stability.

Theorem 5.14 *The null solution of (34) is strongly stable if and only if* $C(\vec{\tau}) < 0$, *or, equivalently,* $c(\vec{\tau}) < 0$ *and* $\gamma_0 < 1$, *where* γ_0 *is defined by (47).*

Finally we note, that both the spectral abscissa and the robust spectral abscissa of (34) are continuous functions of the elements of the system matrices.

5.3 Robust Stabilization by Eigenvalue Optimization

As in Sect. 3, we assume that the system matrices smoothly depend on control or design parameters $p \in \mathbb{R}^{n_p}$, which is made explicit in the description

$$E\dot{x}(t) = A_0(p)x(t) + \sum_{i=1}^{m} A_i(p)x(t - \tau_i). \tag{49}$$

For example, in the feedback interconnection (38)–(39) parameter vector p may arise from a parameterization of matrices $(A_K^i,\ B_K^i,\ C_K^i,\ D_K^i)$.

To impose exponential stability of the null solution of (49), it is necessary to find values of p for which the spectral abscissa is strictly negative. If the achieved stability is required to be *robust against small delay perturbations*, this requirement must be strengthened to the negativeness of the robust spectral abscissa. This brings us to the optimization problem

$$\min_p C(\vec{\tau};\, p). \tag{50}$$

Strongly stabilizing values of p exist if the objective function can be made strictly negative. By Theorem 5.14 the latter can be evaluated as

$$C(\vec{\tau};\, p) = \max(c(\vec{\tau};\, p), C_D(\vec{\tau};\, p)). \tag{51}$$

An alternative approach consists of solving the constrained optimization problem

$$\inf_p c(\vec{\tau};\, p),\ \text{subject to}\ \gamma_0(p) < \gamma, \tag{52}$$

with $\gamma < 1$. If the objective function is strictly negative, then the satisfaction of the constraint implies strong stability. Problem (52) can be solved using the barrier method proposed in Vyhlídal et al. (2010), which is inspired by interior point algorithms, see, e.g., Boyd and Vandenberghe (2004). The first step consists of finding a feasible point, i.e., a set of values for p satisfying the constraint. If the feasible set is

nonempty, such a point can be found by solving

$$\min_p \gamma_0(p). \tag{53}$$

Once a feasible point $p = p_0$ has been obtained, one can solve in the next step the unconstrained optimization problem

$$\min_p \; c(p) - r \log(\gamma - \gamma_0(p)), \tag{54}$$

where $r > 0$ is a small number and γ satisfies

$$\gamma_0(p) < \gamma \leq 1.$$

The second term in (54), the barrier, assures that the feasible set cannot be left when the objective function is decreased in a quasi-continuous way (because the objective function will go to infinity when $\gamma_0 \to \gamma$). If (54) is repeatedly solved for decreasing values of r and with the previous solution as a starting value, a solution of (52) is obtained.

For optimization problem (50) and for subproblems (53) and (54), which are in general not everywhere differentiable but smooth a.e., we use once again the code HANSO (Overton 2009). Note in particular that the switching between the arguments of the maximum operator in (51) is treated in the same way as the switching between individual characteristic root paths when optimizing only the spectral abscissa. The overall algorithm only requires the evaluation of the objective function, as well as its derivatives with respect to the controller parameters, *whenever* it is differentiable. The spectral abscissa can be computed using a spectral discretization, directly extending the approach of Sect. 2.1, followed by Newton corrections. The quantities C_D and γ_0 can be computed using the characterizations in Theorem 5.8, where the (global) maximization problems in (46) and (47) are solved by discretizing the domain $[0,\ 2\pi]^{m-1}$, followed by local corrections. In all cases derivatives with respect to p can be obtained from derivatives of individual eigenvalues or singular values. For more details and expressions we refer to Michiels (2011).

5.4 Examples

We first illustrate the design of a strongly stabilizing controller. Subsequently, we show how the computation of zeros of transfer function (3) can be recast in the computation of characteristic roots of an associated DDAE.

Example 5.15 We consider the system with input delay from Vanbiervliet et al. (2008),

$$\dot{x}(t) = Ax(t) + Bu(t-\tau), \quad y(t) = x(t), \tag{55}$$

where

$$A = \begin{bmatrix} -0.08 & -0.03 & 0.2 \\ 0.2 & -0.04 & -0.005 \\ -0.06 & 0.2 & -0.07 \end{bmatrix}, \quad B = \begin{bmatrix} -0.1 \\ -0.2 \\ 0.1 \end{bmatrix}, \quad \tau = 5. \tag{56}$$

The uncontrolled system is unstable, with spectral abscissa equal to 0.108. We design a stabilizing static controller

$$u(t) = Ky(t), \tag{57}$$

as well as a dynamic controller of the form

$$\begin{cases} \dot{x}_c(t) = A_c x_c(t) + B_c y(t), \\ u(t) \ = C_c x_c(t) + D_c y(t), \quad x_c(t) \in \mathbb{R}^{n_c}, \end{cases} \tag{58}$$

using the approach of Sect. 5.3. More precisely we treat (55) and (57), respectively (55) and (58), as a system of DDAEs, with (pseudo)state $[x^T \ u^T \ y^T]^T$, respectively $[x^T \ x_c^T \ u^T \ y^T]^T$, while we set $p = \text{vec}\, K$, respectively

$$p = \text{vec} \begin{bmatrix} A_c & B_c \\ C_c & D_c \end{bmatrix}.$$

Since the transfer function from u to y in (55) is strictly proper, the robust spectral abscissa equals the spectral abscissa, and optimization problems (50) and (52) reduce to the (unconstrained) minimization of the spectral abscissa. The resulting optimized spectrum is displayed in Fig. 5 for the static controller and for a dynamic controller of order $n_c = 2$. Note that the additional degrees of freedom in the dynamic controller lead to a further reduction of the spectral abscissa.

Next we assume that the measured output of system (55) is instead given by

$$\tilde{y}(t) = x(t) + \begin{bmatrix} 3 \\ 4 \\ 1 \end{bmatrix} u(t - 2.5) + \begin{bmatrix} 2/5 \\ -2/5 \\ -2/5 \end{bmatrix} u(t - 5), \tag{59}$$

for which we design a static controller,

$$u(t) = D_c \tilde{y}(t).$$

As a main difference with the previous example, there are two non-trivial feedthrough terms in the system model, which are both delayed. By a combination of this model and the control law, the closed loop system is no longer of retarded type. Solving optimization problem (50) leads us to

$$C = -0.0309, \quad D_c = [0.0409 \ \ 0.0612 \ \ 0.3837]. \tag{60}$$

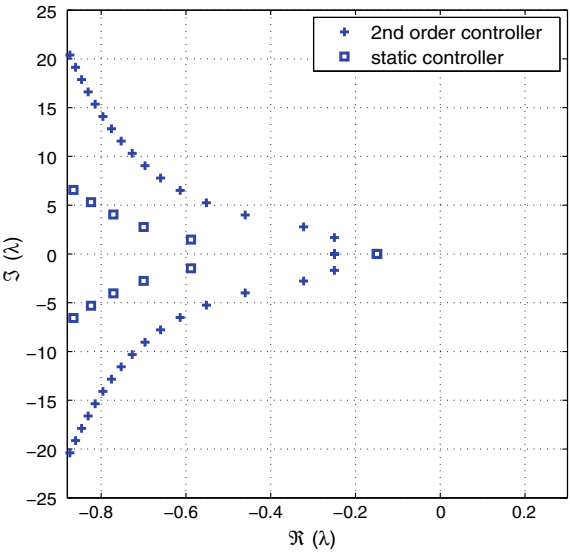

Fig. 5 Characteristic roots of controlled system (55)–(56), corresponding to a minimum of the spectral abscissa function, for static controller (57) (boxes) and for dynamic controller (58) of order two (pluses)

The computed rightmost characteristic roots of the closed-loop system are given by

$$\begin{aligned}\lambda_1 &= -0.0309,\\ \lambda_{2,3} &= -0.0309 \pm 0.0001\mathrm{i},\\ \lambda_{4,5} &= -0.3336 \pm 2.3789\mathrm{i},\\ \lambda_{6,7} &= -0.3499 \pm 4.8863\mathrm{i}.\end{aligned}$$

They indicate that the optimum is characterized by a rightmost characteristic root of multiplicity three, which must be non-semisimple because of the use of a single control input. Note that due to the high sensitivity of such roots (Michiels et al. 2017), a very accurate replication using an a-posteriori spectrum computation is not possible.

The presence of three rightmost roots (counting multiplicity) may sound counter-intuitive because the number of degrees of freedom in the controller is also three. The explanation is that we are in a situation where $C_D \geq c$. In fact, the optimum of (50) is characterized by an equality between C_D and the spectral abscissa c. Hence, in the optimum we have four conflicting objectives: the three eigenvalues constituting the multiple root, and the behavior of high frequency characteristic roots, captured by quantity C_D. In the left panel of Fig. 6 we show the rightmost characteristic roots corresponding to the minimum of the robust spectral abscissa (60). The dotted line corresponds to $\Re(\lambda) = c_D$, the dashed line to $\Re(\lambda) = C_D$. In order to illustrate that we indeed have $c = C_D$, we depict in the right panel of Fig. 6 the rightmost characteristic roots after perturbing the delay value 2.5 in (59) to 2.51.

When we solve instead the constrained optimization problem (52) with the default parameters $r = 10^{-3}$ and $\gamma = 1 - 10^{-3}$ in the relaxation (54), we arrive at the

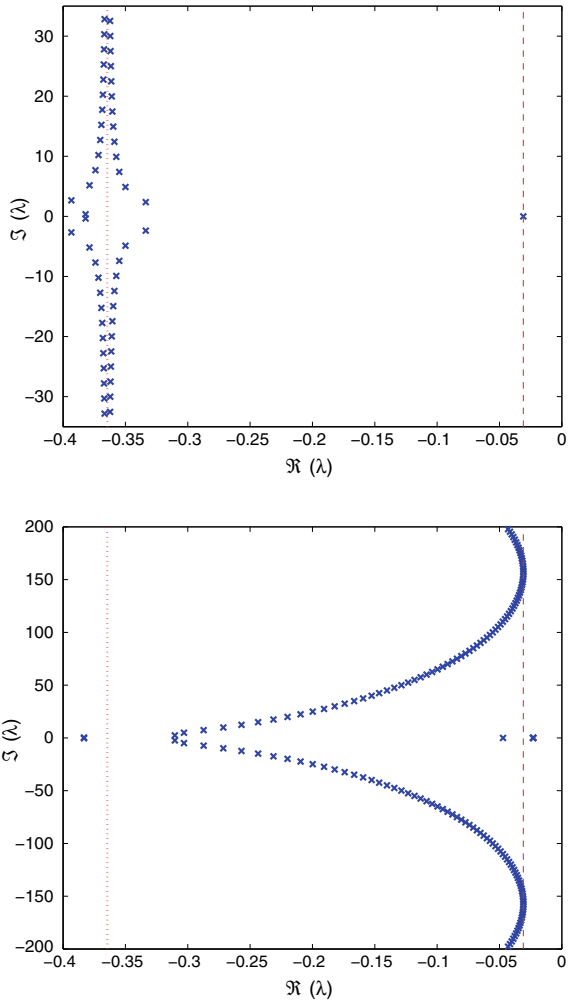

Fig. 6 (Top) Characteristic roots corresponding to the minimum of the robust spectral abscissa of the second example (55) and (59), using a static controller. The rightmost characteristic roots, $\lambda \approx -0.0309$, has multiplicity three. (Bottom) Effect on the characteristic roots of a perturbation of the delays (2.5, 5) in (59) to (2.51, 5)

controller gain $D_c = [0.0249\ 0.1076\ 0.3173]$. Compared to (60), where we had $C = c = C_D$, a further reduction of the spectral abscissa to $c = -0.0345$ has been achieved, at the price of an increased value of C_D (equal to -0.00602). This is expected because the constraint $\gamma_0 < 1$ imposes robustness of stability, yet no bound on the exponential decay rate of the solutions.

Example 5.16 A transmission zero of system (1) is a number $z_0 \in \mathbb{C}$ such that $G(z_0) = 0$. In the time-domain the meaning is as follows. If an exponentially stable system is excited by signal

$$\zeta(t) = \underline{\zeta} e^{z_0 t}, \tag{61}$$

then the stationary response in the output η is identically zero, for any $\underline{\zeta} \in \mathbb{C}^{n_\zeta}$. This interpretation is at the basis of the computation of transmission zeros. Due to the separation principle in the frequency domain, the stationary response to excitation (61) takes the form

$$x(t) = \underline{x}e^{z_0 t}, \ \eta(t) = \underline{\eta}e^{z_0 t}.$$

Substituting these functions in (1) and requiring that $\eta \equiv 0$ brings us to

$$\begin{bmatrix} z_0 I - A_0 - \sum_{i=1}^{m} A_i e^{-z_0 \tau_i} & -B \\ C & De^{-z_0 \tau_{m+1}} \end{bmatrix} \begin{bmatrix} \underline{x} \\ \underline{\zeta} \end{bmatrix} e^{z_0 t} = 0.$$

The 2-by-2 block matrix in the left-hand side can be interpreted as the characteristic matrix of a DDAE, and, accordingly, its characteristic roots are the transmission zeros. The extension to model (34) is straightforward.

Transmission zeros play a central role in applications related to vibration control. Signal shapers and vibration absorbers are tuned in such a way that the transfer function from the location where undesired vibrations enter the system to the location where vibrations need to be annihilated, has transmission zeros at the dominant frequencies. For the design and implementation of novel classes of signal shapers and vibration absorbers that explicitly use delays as controller parameters, and for the use of DDAE models to describe the overall system, we refer to Pilbauer (2017) and the references therein.

5.5 *Note on the Strong $\mathcal{H}_2$ and $\mathcal{H}_\infty$ Norm*

Similarly to the spectral abscissa, the $\mathcal{H}_2$ and $\mathcal{H}_\infty$ system norms of DDAEs suffer from a fragility problem, in the sense of being potentially sensitive to infinitesimal delay perturbations. The latter cannot be excluded from an application point of view. Before we analyze the problem and present robustified measures, we introduce some notation and motivating examples. We denote by $\hat{G}$ the transfer function of (34),

$$\hat{G}(\lambda) := C \left(\lambda E - A_0 - \sum_{i=1}^{m} A_i e^{-\lambda \tau_i} \right)^{-1} B.$$

We also introduce the corresponding *asymptotic transfer function* $\hat{G}_a$,

$$\hat{G}_a(s) := C_2 \left(I - \sum_{i=1}^{m} A_i^{(22)} e^{-\lambda \tau_i} \right)^{-1} B_2.$$

It can be interpreted as the transfer function of delay difference equation

$$\begin{cases} x_2(t) = \sum_{i=1}^{m} A_i^{(22)} x_2(t-\tau_i) + B_2\zeta(t), \\ \eta(t) = C_2 x_2(t), \end{cases} \tag{62}$$

obtained by setting $x_1 = 0$ in the second equation of (40). It describes the asymptotic behavior of $\hat{G}(\lambda)$ for $|\lambda| \to \infty$ in the closed right half plane. The following property is proven in Gumussoy and Michiels (2011).

Proposition 5.17 *For all $\gamma > 0$, there exists a number $\Omega > 0$ such that $\left\| \hat{G}(i\omega) - \hat{G}_a(i\omega) \right\|_2 < \gamma$ for all $\omega > \Omega$.*

With the following example we illustrate that functions

$$\left(\mathbb{R}_0^+\right)^m \ni \vec{\tau} \mapsto \left\| \hat{G}(\cdot;\vec{\tau}) \right\|_{\mathcal{H}_2}, \quad \left(\mathbb{R}_0^+\right)^m \ni \vec{\tau} \mapsto \left\| \hat{G}(\cdot;\vec{\tau}) \right\|_{\mathcal{H}_\infty}$$

may not be continuous, even if the system is strongly stable, and that this phenomenon is related to the behavior of the asymptotic transfer function.

Example 5.18 We consider system (34), already in the form (40) with $m = 2$ and matrices $E^{(11)} = 1$, $A_0^{(11)} = -10$, $A_0^{(12)} = \begin{bmatrix} 1 & 1 \end{bmatrix}$, $A_0^{21} = \begin{bmatrix} 0 & 0 \end{bmatrix}^T$,

$$\left[\begin{array}{c|c} A_1^{(11)} & A_1^{(12)} \\ \hline A_1^{(21)} & A_1^{(22)} \end{array}\right] = \left[\begin{array}{c|cc} 0 & 0 & 0 \\ \hline 0 & \frac{1}{4} & 0 \\ 0 & -1 & \frac{1}{4} \end{array}\right], \quad \left[\begin{array}{c|c} A_2^{(11)} & A_2^{(12)} \\ \hline A_2^{(21)} & A_2^{(22)} \end{array}\right] = \left[\begin{array}{c|cc} 0 & 0 & 0 \\ \hline 0 & \frac{1}{8} & \frac{1}{8} \\ 0 & 1 & \frac{1}{8} \end{array}\right],$$
$$\left[\begin{array}{c} B_1 \\ \hline B_2 \end{array}\right] = \left[\begin{array}{c} 100 \\ \hline 1 \\ 0 \end{array}\right], \quad \left[\begin{array}{c|c} C_1 & C_2 \end{array}\right] = \left[\begin{array}{c|cc} 1 & 0 & 1 \end{array}\right]. \tag{63}$$

The system is exponentially stable for all delay values, and thus strongly stable. Due to its tridiagonal structure, its spectrum namely consists of eigenvalue $\lambda = -10$, supplemented with the spectrum of (62), which is confined to the open left half plane because $\gamma_0 = 0.625 < 1$.

We now analyze the system norms from input ζ to output η. In Fig. 7 we show in the left the transfer function $\hat{G}$ and in the right the asymptotic transfer function $\hat{G}_a$, evaluated on the imaginary axis, for $\lambda = \mathrm{i}\omega$. Notice their matching at large frequencies, in accordance with Proposition 5.17. For $\vec{\tau} = (1, 1)$ there is clearly no feedthrough from input to output, inducing a finite $\mathcal{H}_2$ norm. Let us now consider rationally independent delays $\vec{\tau} = (1, 1 + \pi/\upsilon)$ with $\upsilon \in \mathbb{N}$. For $\upsilon = 50$ we see that functions $\hat{G}$ and $\hat{G}_a$ do not tend to zero as $\omega \to \infty$. If υ tends to infinity, the deviation from nominal delays $(1, 1)$ tends to zero. However, the $\mathcal{H}_2$ norms of $\hat{G}$ and $\hat{G}_a$ remain unbounded, while the significant mismatch of the transfer functions and the corresponding transfer functions for the limit $\vec{\tau} = (1, 1)$ only shifts towards higher frequencies. This is visualized in the figure by comparing the cases where $\upsilon = 50$ and $\upsilon = 200$. Thus, the $\mathcal{H}_2$ norm of $\hat{G}$ is not continuous at the nominal delays $\vec{\tau} = (1, 1)$. Its $\mathcal{H}_\infty$ norm is continuous and characterized by the peak gain reached for $\omega = 0$.

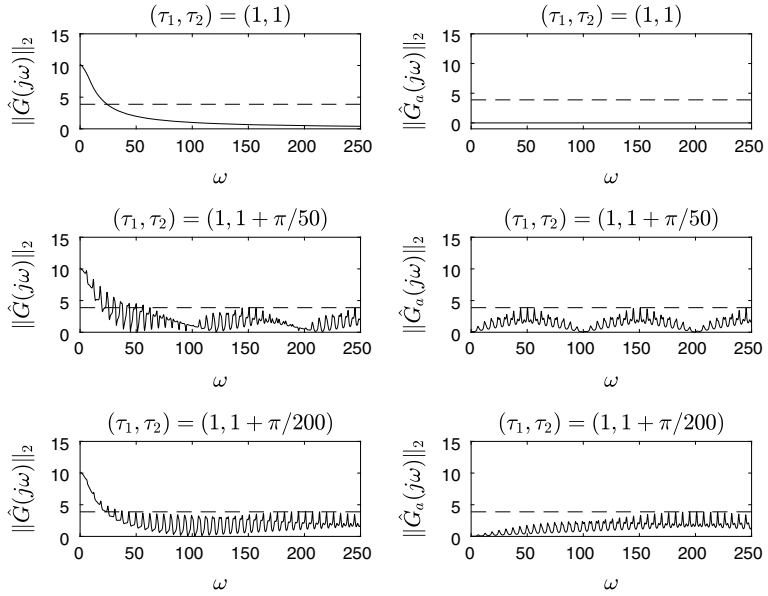

Fig. 7 Maximum singular value of the transfer function (left) and asymptotic transfer function (right) of the system in Example 5.18 as a function of $s = \mathrm{i}\omega$, for three cases: $\vec{\tau} = (1, 1)$ (top), $\vec{\tau} = (1, 1 + \pi/50)$ (middle) and $\vec{\tau} = (1, 1 + \pi/200)$ (bottom). The dashed line indicates the strong $\mathcal{H}_\infty$ norm of $\hat{G}_a$

Let us now consider other numerical values for the input matrix B, while keeping the other system matrices:

$$B = \left[\frac{B_1}{B_2}\right] = \left[\begin{array}{c} 25 \\ \hline 1 \\ 0 \end{array}\right]. \tag{64}$$

In Fig. 8 we display again the transfer functions. With the modified input matrix, not only the $\mathcal{H}_2$ norm is discontinuous at nominal delays $(1, 2)$, but also the $\mathcal{H}_\infty$ norm.

The possible discontinuity of the system norms brings us to the following robustified counter parts, which explicitly take into account infinitesimal delay perturbations.

Definition 5.19 The strong $\mathcal{H}_2$ and strong $\mathcal{H}_\infty$ norm of $\hat{G}$ are defined as

$$\begin{aligned} |||\hat{G}(\cdot; \vec{\tau})|||_{\mathcal{H}_2} &:= \lim_{\epsilon \to 0+} \sup\{\|\hat{G}(\cdot; \vec{\tau}_\epsilon)\|_{\mathcal{H}_2} : \vec{\tau}_\epsilon \in \mathcal{B}(\vec{\tau}, \epsilon)\}, \\ |||\hat{G}(\cdot; \vec{\tau})|||_{\mathcal{H}_\infty} &:= \lim_{\epsilon \to 0+} \sup\{\|\hat{G}(\cdot; \vec{\tau}_\epsilon)\|_{\mathcal{H}_\infty} : \vec{\tau}_\epsilon \in \mathcal{B}(\vec{\tau}, \epsilon)\}, \end{aligned}$$

with $\mathcal{B}$ given by (45).

The strong $\mathcal{H}_2$ and $\mathcal{H}_\infty$ norm of $\hat{G}_a$ are defined in a similar way. In order to provide mathematical characterizations of the strong norms, we first introduce matrix poly-

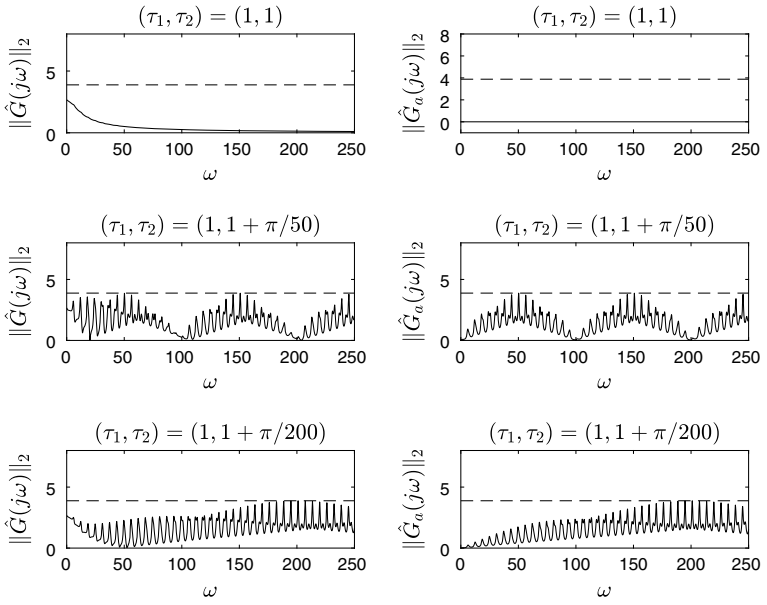

Fig. 8 Maximum singular value of the transfer function (left) and asymptotic transfer function (right) of the system in Example 5.18, with modified input matrix (64), as a function of $s = \mathrm{i}\omega$, for three cases: $\vec{\tau} = (1, 1)$ (top), $\vec{\tau} = (1, 1 + \pi/50)$ (middle) and $\vec{\tau} = (1, 1 + \pi/200)$ (bottom). The dashed line indicates the strong $\mathcal{H}_\infty$ norm of $\hat{G}_a$

nomials $P_{k_1,\ldots,k_m}$, with $k_i \in \mathbb{Z}^+$, $i = 1, \ldots, m$, which are recursively defined through the following expressions:

$$P_{0,\ldots,0} := I, \tag{65}$$

$$\begin{aligned} P_{k_1,\ldots,k_m} := {} & A_1^{(22)} P_{k_1-1,k_2,\ldots,k_m} + A_2^{(22)} P_{k_1,k_2-1,k_3,\ldots,k_m} \\ & + \ldots + \hat{A}_m^{(22)} P_{k_1,k_2,\ldots,k_{m-1},k_m-1} \end{aligned} \tag{66}$$

and

$$P_{k_1,\ldots,k_m} := 0 \text{ if any } k_i \in \mathbb{Z}^-, i = 1, \ldots, m. \tag{67}$$

For instance, for $m = 2$ and $k_1 + k_2 \leq 2$ these matrix polynomials are

$$\begin{aligned} & P_{0,0} = I, \\ & P_{1,0} = A_1^{(22)}, \ P_{0,1} = A_2^{(22)}, \\ & P_{2,0} = A_1^{(22)} A_1^{(22)}, \ P_{1,1} = A_1^{(22)} A_2^{(22)} + A_2^{(22)} A_1^{(22)}, \ P_{0,2} = A_2^{(22)} A_2^{(22)}, \end{aligned}$$

while we also have

$$P_{2,1} = A_1^{(22)} A_1^{(22)} A_2^{(22)} + A_1^{(22)} A_2^{(22)} A_1^{(22)} + A_2^{(22)} A_1^{(22)} A_1^{(22)}.$$

Hence $P_{k_1,\ldots,k_m}$ is the sum of all monomials of order k_i in matrix $A_i^{(22)}$, for all $i = 1, \ldots, m$. We can now formulate a characterization of the strong norms of the asymptotic transfer function.

Proposition 5.20 (Gomez et al. 2010, Proposition 1) *Assume that system* (34) *is strongly stable. Then its asymptotic transfer function* $\hat{G}_a$ *satisfies*

$$\| \hat{G}_a \|_{\mathcal{H}_\infty} = \max_{\vec{\theta} \in [0,\ 2\pi]^m} \left\| C_2 \left(I - \sum_{i=1}^{m} A_i^{(22)} e^{-i\theta_i} \right)^{-1} B_2 \right\|_2 . \tag{68}$$

If conditions

$$C_2 P_{k_1,\ldots,k_m} B_2 = 0, \quad \forall (k_1, \ldots, k_m) \in \left(\mathbb{Z}^+\right)^m : \sum_{i=1}^{m} k_i < mn \tag{69}$$

are satisfied, with multi-powers $P_{k_1,\ldots,k_m}$ *defined by* (65)-(67)*, then it holds that* $\|G_a\|_{\mathcal{H}_2} = 0$*. Otherwise, it holds that* $\|G_a\|_{\mathcal{H}_2} = +\infty$*.*

It is important to point out that the strong norms of the asymptotic transfer function do not depend on the delay values. We can now state the corresponding results for transfer function $\hat{G}$.

Proposition 5.21 (Gomez et al. 2010, Proposition 2) *If system* (34) *is strongly stable, then its transfer function* $\hat{G}$ *satisfies*

$$\| \hat{G}(\cdot; \vec{\tau}) \|_{\mathcal{H}_\infty} = \max \left\{ \| \hat{G}(\cdot; \vec{\tau}) \|_{\mathcal{H}_\infty}, \| \hat{G}_a \|_{\mathcal{H}_\infty} \right\} \tag{70}$$

and

$$\|\hat{G}(\cdot; \vec{\tau})\|_{\mathcal{H}_2} = \begin{cases} \| \hat{G}(\cdot; \vec{\tau}) \|_{\mathcal{H}_2} < +\infty, & \text{if (69) is satisfied,} \\ +\infty, & \text{otherwise.} \end{cases}$$

Furthermore, function $\left(\mathbb{R}_0^+\right)^m \ni \vec{\tau} \mapsto \|\hat{G}(\cdot; \vec{\tau})\|_{\mathcal{H}_\infty}$ *is continuous whenever* (34) *is strongly stable. Function* $\left(\mathbb{R}_0^+\right)^m \ni \vec{\tau} \mapsto \|\hat{G}(\cdot; \vec{\tau})\|_{\mathcal{H}_2}$ *is continuous whenever* (34) *is strongly stable and the strong* $\mathcal{H}_2$ *norm is finite.*

Example 5.22 We revisit Example 5.18 and consider nominal delay values $(\tau_1, \tau_2) = (1, 1)$. By evaluating (68) we arrive at $\|\hat{G}_a\|_{\mathcal{H}_\infty} = 3.88$, whose corresponding level sets are the dashed horizontal lines in Figs. 7 and 8. Because we have

$$C_2 A_1^{(22)} B_2 = -1, \ C_2 A_2^{(22)} B_2 = 1,$$

the conditions (69) are not satisfied, implying $\|G_a\|_{\mathcal{H}_2} = +\infty$.

For the first choice of B, as in (63), the maximum in the right-hand side of (70) is attained by the first term, hence, the strong $\mathcal{H}_\infty$ norm is reached at a finite frequency,

here $\omega = 0$. For the second choice (64), it is reached by the second term, hence, $|||\hat{G}|||_{\mathcal{H}_\infty} = |||\hat{G}_a|||_{\mathcal{H}_\infty} = 3.88$. Obviously, we have in both cases $|||G|||_{\mathcal{H}_2} = +\infty$.

The computation and subsequent optimization of the strong $\mathcal{H}_\infty$ norm as in Gumussoy and Michiels (2011) is based on expression (70), where in a first phase (68) is evaluated using a combination of gridding and local correction. Here it is important to note that the number of nonzero coefficient matrices $A_i^{(22)}$ is typically very small in applications, as they all correspond to the presence of a control loop along which high frequency modes are not damped. In the second phase, an extension of the level-set algorithm, described in Sect. 2.2 and illustrated with Fig. 1, is used to compute the nominal $\mathcal{H}_\infty$ norm, provided it is larger than $|||\hat{G}_a|||_{\mathcal{H}_\infty}$. For this, the latter norm is used as initial value for the level. Derivatives of the objective function (70) with respect to controller parameters are obtained from derivatives of corresponding active eigenvalues or singular values.

We now address the $\mathcal{H}_2$ norm computation. With several examples, including Examples 5.2 and 5.18, we illustrated that a DDAE of the form (34) may hide nontrivial feedthrough terms, hence after checking strong stability it should be determined first whether the strong $\mathcal{H}_2$ norm is finite. An important property of the necessary and sufficient condition (69), derived in Gomez et al. (2020) using a multi-dimensional generalization of the Cayley-Hamilton theorem, is that this involves checking only finitely many equalities. However, the number of equalities to check has an exponential growth as a function of the number of delays m. In response to this, it can be noted that conditions

$$\begin{aligned} CB &= 0, \\ CA_{\sigma_1} \cdots A_{\sigma_k} B &= 0, \ \forall k \in \mathbb{Z}^+, \forall \sigma_i \in \{1, \ldots, m\}, \ i = 1, \ldots, k \end{aligned} \tag{71}$$

imply that $CP_{k_1,\ldots,k_m}B = 0$ for any m-tuple $(k_1, \ldots, k_m)$, and, hence, that finiteness criterion (69) is satisfied. In Gomez et al. (2010) it is shown that checking sufficient condition (71) can be done with an algorithm having significantly better scalability properties in terms of both the dimension of the system and the number of delays. It is also shown that the satisfaction of (71) is equivalent to the existence of a simultaneous block triangularization of the matrices of delay difference equation (62). The latter is instrumental to a special regularization procedure that allows to transform DDAE (34) to a neutral equation with the same transfer matrix, without any need for differentiation of inputs or outputs. This transformation enables to compute the strong $\mathcal{H}_2$ norm using an established approach grounded in Lyapunov matrices (Jarlebring et al. 2011), thereby directly extending Theorem 1 and the related algorithms. For further reading we refer to Gomez and Michiels (2019a), Gomez et al. (2010, 2020).

6 Concluding Remarks

An eigenvalue based solution to the robust control of linear time-delay systems has been presented. Because any controller characterized by a finite number of parameters can be seen as a structured, reduced-order controller, a direct optimization approach has been taken. Its main advantages are two-fold. First, the methods are generally applicable. The extension of model (1) towards DDAE models allows to consider both retarded and neutral type stand-alone and interconnected systems, with discrete delays in states, control input, sensors outputs, and in the inputs and outputs used to describe the robustness and performance specifications. As a second advantage, the approach is not conservative in the sense that a stabilizing or optimal fixed-structure $\mathcal{H}_2 - \mathcal{H}_\infty$ controller can be computed whenever it exists, in contrast to approaches inferred from sufficient (but not necessary) conditions for a stabilizing or a guaranteed cost controller. As a price to pay for these beneficial properties, the optimization problems encountered in Sects. 3 and 5.3 are in general non-convex, hence, there is no guarantee that the computed optima found by the presented local optimization algorithms are global.

The eigenvalue based framework has recently been extended to the robust stability analysis and stabilization of linear time-periodic systems with delay (Michiels and Fenzi 2020; Borgioli et al. 2020), the $\mathcal{H}_2$ norm analysis of such systems (Michiels and Gomez 2020), and it has been applied to problems from machining (Hajdu et al. 2020). It has also been adopted to the design of prediction based controllers, see, e.g., Zhou et al. (2019) and the references therein.

Software tools for solving the analysis and synthesis problems discussed in this article, as well as a benchmark data, are available at

`http://twr.cs.kuleuven.be/research/software/delay-control/`.

They have been integrated in the software package TDS-CONTROL (Appeltans and Michiels 2022).

References

Appelmans, P., & Michiels, W. (2022). TDS-CONTROL: A MATLAB package for the analysis and controller-design of time-delay systems. In *Proceedings of the 18th IFAC Workshop on Control Applications of Optimization*, Gif-sur-Yvette, France.

Avellar, C. E., & Hale, J. K. (1980). On the zeros of exponential polynomials. *Journal of Mathematical Analysis and Applications, 73*, 434–452.

Borgioli, F., & Michiels, W. (2020). A novel method to compute the structured distance to instability for combined uncertainties on delays and system matrices. *IEEE Transactions on Automatic Control, 65*(4), 1747–1754.

Borgioli, F., Michiels, W., Lu, D., & Vandereycken, B. (2019). A globally convergent method to compute the real stability radius for time-delay systems. *Systems & Control Letters, 127*, 44–51.

Borgioli, F., Hajdu, D., Insperger, T., Stépán, G., & Michiels, W. (2020). Pseudospectral method for assessing stability robustness for linear time-periodic delayed dynamical systems. *International Journal for Numerical Methods in Engineering*.

Boyd, S., & Balakrishnan, V. (1990). A regularity result for the singular values of a transfer matrix and a quadratically convergent algorithm for computing its $\mathcal{L}_\infty$-norm. *Systems & Control Letters, 15*, 1–7.

Boyd, S., & Vandenberghe, L. (2004). *Convex optimization*. Cambridge University Press.

Breda, D. (2023). Pseudospectral Methods for the Stability Analysis of Delay Equations. Part I: the Infinitesimal Generator Approach. methods and applications. In D. Breda (Ed.) *Controlling Delayed Dynamics: Advances in Theory, Methods and Applications, CISM Lecture Notes* (pp. 65–94). Wien-New York: Springer.

Breda, D. (2023). Pseudospectral Methods for the Stability Analysis of Delay Equations. Part II: the Solution Operator Approach. methods and applications. In D. Breda (Ed.) *Controlling Delayed Dynamics: Advances in Theory, Methods and Applications, CISM Lecture Notes* (pp. 95–116). Wien-New York: Springer.

Breda, D., Maset, S., & Vermiglio, R. (2005). Pseudospectral differencing methods for characteristic roots of delay differential equations. *SIAM Journal on Scientific Computing, 27*(2), 482–495.

Breda, D., Maset, S., & Vermiglio, R. (2009). TRACE-DDE: a tool for robust analysis and characteristic equations for delay differential equations. In *Topics in time-delay systems*, *Lecture Notes in Control and Information Sciences* (Vol. 388, pp. 145–155). Springer.

Bruinsma, N. A., & Steinbuch, M. (1990). A fast algorithm to compute the $\mathcal{H}_\infty$-norm of a transfer function matrix. *Systems & Control Letters, 14*, 287–293.

Burke, J. V., Lewis, A. S., & Overton, M. L. (2005). A robust gradient sampling algorithm for nonsmooth, nonconvex optimization. *SIAM Journal on Optimization, 15*(3), 751–779.

Burke, J. V., Henrion, D., Lewis, A. S., Overton, M. L. (2006). HIFOO - a MATLAB package for fixed-order controller design and H-infinity optimization. In *Proceedings of the 5th IFAC Symposium on Robust Control Design*, Toulouse, France.

Curtain, R. F., & Zwart, H. (1995). *An introduction to infinite-dimensional linear systems theory*, *Texts in Applied Mathematics* (Vol. 21). Springer.

Dileep, D., Van Parys, R., Pipeleers, G., Hetel, L., Richard, J.-P., & Michiels, W. (2020). Design of robust decentralised controllers for MIMO plants with delays through network structure exploitation. *The International Journal of Control, 93*(10), 2275–2289.

Du, N. H., Linh, V. H., Mehrmann, V., & Thuan, D. D. (2013). Stability and robust stability of linear time-invariant delay differential-algebraic equations. *SIAM Journal on Matrix Analysis and Applications, 34*(4), 1631–1654.

Engelborghs, K., Luzyanina, T., & Roose, D. (2002). Numerical bifurcation analysis of delay differential equations using DDE-BIFTOOL. *ACM Transactions on Mathematical Software, 28*(1), 1–24.

Fridman, E. (2002). Stability of linear descriptor systems with delay: A Lyapunov-based approach. *Journal of Mathematical Analysis and Applications, 273*, 24–44.

Gomez, M. A., & Michiels, W. (2019a). Analysis and computation of the $\mathcal{H}_2$ norm of delay differential algebraic equations. *IEEE Transactions on Automatic Control, 65*(5), 2192–2199.

Gomez, M. A., & Michiels, W. (2019b). Characterization and optimization of the smoothed spectral abscissa for time-delay systems. *The International Journal of Robust and Nonlinear Control, 29*(13), 4402–4418.

Gomez, M. A., Egorov, A., Mondié, S., & Michiels, W. (2019). Optimization of the $\mathcal{H}_2$ norm for single-delay systems, with application to control design and model approximation. *IEEE Transactions on Automatic Control, 64*(2), 804–811.

Gomez, M. A., Jungers, R. M., & Michiels, W. (2020). On the m-dimensional Cayley-Hamilton theorem and its application to an algebraic decision problem inferred from the $\mathcal{H}_2$ norm analysis of delay systems. *Automatica, 113*, 108761.

Gomez, M. A., Jungers, R. M. & Michiels, W. (2010). On the strong $\mathcal{H}_2$ norm of differential algebraic systems with multiple delays: finiteness criteria, regularization and computation. *IEEE Transactions on Automatic Control*. Accepted for publication.

Gu, K., Kharitonov, V. L., & Chen, J. (2003). *Stability of time-delay systems*. Birkhauser.

Gumussoy, S., & Michiels, W. (2010). A predictor - corrector type algorithm for the pseudospectral abscissa computation of time-delay systems. *Automatica, 46*(4), 657–664.

Gumussoy, S., & Michiels, W. (2011). Fixed-order H-infinity control for interconnected systems using delay differential algebraic equations. *SIAM Journal on Control and Optimization, 49*(5), 2212–2238.

Güttel, S., Van Beeumen, R., Meerbergen, K., & Michiels, W. (2014). NLEIGS: A class of fully rational Krylov methods for nonlinear eigenvalue problems. *SIAM Journal on Scientific Computing, 36*(6), A2842–A2864.

Ha, P., & Mehrmann, V. (2012). Analysis and reformulation of linear delay differential-algebraic equations. *The Electronic Journal of Linear Algebra, 23*, 703–730.

Hajdu, D., Borgioli, F., Michiels, W., Insperger, T., & Stépán, G. (2020). Robust stability of milling operations based on pseudospectral approach. *International Journal of Machine Tools and Manufacture, 149*, 103516.

Hale, J. K., & Verduyn Lunel, S. M. (1993). *Introduction to functional differential equations*, *Applied Mathematical Sciences* (Vol. 99). Springer.

Hale, J. K., & Verduyn Lunel, S. M. (2002). Strong stabilization of neutral functional differential equations. *IMA Journal of Mathematical Control and Information, 19*, 5–23.

Jarlebring, E., Meerbergen, K., & Michiels, W. (2010). A Krylov method for the delay eigenvalue problem. *SIAM Journal on Scientific Computing, 32*(6), 3278–3300.

Jarlebring, E., Vanbiervliet, J., & Michiels, W. (2011). Characterizing and computing the $\mathcal{H}_2$ norm of time-delay systems by solving the delay Lyapunov equation. *IEEE Transactions on Automatic Control, 56*, 814–825.

Jarlebring, E., Bennedich, M., Mele, G., Ringh, E., & Upadhyaya, P. (2018). NEP-PACK: A julia package for nonlinear eigenproblems - v0.2.

Kharitonov, V., & Plischke, E. (2006). Lyapunov matrices for time-delay systems. *Systems & Control Letters, 55*(9), 697–706.

Lewis, A., & Overton, M. L. (2009). Nonsmooth optimization via BFGS. Available from `http://cs.nyu.edu/overton/papers.html`.

Michiels, W. (2019). Control of linear systems with delays (pp. 1–7). London: Springer. ISBN 978-1-4471-5102-9.

Michiels, W. (2011). Spectrum-based stability analysis and stabilisation of systems described by delay differential algebraic equations. *IET Control Theory & Applications, 5*, 1829–1842.

Michiels, W., Boussaada, I., & Niculescu, S.-I. (2017). An explicit formula for the splitting of multiple eigenvalues for nonlinear eigenvalue problems and connections with the linearization for the delay eigenvalue problem. *SIAM Journal on Matrix Analysis and Applications, 38*(2), 599–620.

Michiels, W., Engelborghs, K., Roose, D., & Dochain, D. (2002). Sensitivity to infinitesimal delays in neutral equations. *SIAM Journal on Control and Optimization, 40*(4), 1134–1158.

Michiels, W., & Fenzi, L. (2021). Spectrum-based stability analysis and stabilization of a class of time-periodic time delay systems. *SIAM Journal on Matrix Analysis and Applications, 5*(16), 1829–1842.

Michiels, W., & Gomez, M. A. (2020). On the dual linear periodic time-delay system: Spectrum and Lyapunov matrices, with application to $\mathcal{H}_2$ analysis and balancing. *The International Journal of Robust and Nonlinear Control, 30*(10), 3906–3922.

Michiels, W., & Gumussoy, S. (2010). Characterization and computation of H-infinity norms of time-delay systems. *SIAM Journal on Matrix Analysis and Applications, 31*(4), 2093–2115.

Michiels, W., & Niculescu, S.-I. (2014). *Stability and stabilization of time-delay systems. An eigenvalue based approach*, 2nd edn. SIAM.

Michiels, W., & Vyhlídal, T. (2005). An eigenvalue based approach to the robust stabilization of linear time-delay systems of neutral type. *Automatica, 41*(6), 991–998.

Michiels, W., Vyhlídal, T., & Zítek, P. (2010). Control design for time-delay systems based on quasi-direct pole placement. *Journal of Process Control, 20*(3), 337–343.

Michiels, W., Vyhlídal, T., Ziték, P., Nijmeijer, H., & Henrion, D. (2009). Strong stability of neutral equations with an arbitrary delay dependency structure. *SIAM Journal on Control and Optimization, 48*(2), 763–786.

Michiels, W., & Zhou, B. (2019). Computing delay lyapunov matrices and $\mathcal{H}_2$ norms for large-scale problems. *SIAM Journal on Matrix Analysis and Applications, 40*(3), 845–869.

Niculescu, S.-I. (2001). *Delay effects on stability. A robust control approach*, *Lecture Notes in Control and Information Sciences* (Vol. 269). Springer.

Overton, M. (2009). HANSO: a hybrid algorithm for nonsmooth optimization. `http://cs.nyu.edu/overton/software/hanso/`.

Pilbauer, D. (2017). *Spectral Methods in Vibration Suppression Control Systems with Time Delays*. Ph.D. thesis, Double Doctorate Chech Technical University in Prague - KU Leuven.

Pontes Duff, I., Poussot-Vassal, C., & Seren, C. (2018). H_2-optimal model approximation by input/output-delay structured reduced order models. *Systems & Control Letters, 117,* 60 – 67.

Saad, Y. (1992). *Numerical methods for large eigenvalue problems*. Manchester University Press.

Sieber, J., Engelborghs, K., Luzyanina, T., Samey, G., & Roose, D. (2016). DDE-BIFTOOL manual - bifurcation analysis of delay differential equations - v3.1.1.

Sipahi, R., Niculescu, S. I., Abdallah, C. T., Michiels, W., & Gu, K. (2011). Stability and stabilization of systems with time delay. *IEEE Control Systems Magazine, 31*(38–65), 3278–3300.

Van Beeumen, R., Meerbergen, K., & Michiels, W. (2015). Compact rational Krylov methods for nonlinear eigenvalue problems. *SIAM Journal on Matrix Analysis and Applications, 36*(2), 820–838.

Vanbiervliet, J., Vandereycken, B., Michiels, W., & Vandewalle, S. (2008). A nonsmooth optimization approach for the stabilization of time-delay systems. *ESAIM: Control, Optimisation and Calculus of Variations, 14*(3), 478–493.

Vanbiervliet, J., Michiels, W., & Vandewalle, S. (2009a). Smooth stabilization and optimal $\mathcal{H}_2$ design. In *Proceedings of the IFAC Workshop on Control Applications of Optimization*, Jyväskylä, Finland.

Vanbiervliet, J., Vandereycken, B., Michiels, W., Vandewalle, S., & Diehl, M. (2009). The smoothed spectral abscissa for robust stability optimization. *SIAM Journal on Optimization, 20*(1), 156–171.

Vanbiervliet, J., Michiels, W., & Jarlebring, E. (2011). Using spectral discretisation for the optimal $\mathcal{H}_2$ design of time-delay systems. *International Journal of Control, 84*(2), 228–241.

Villafuerte, R., Mondié, S., & Garrido, R. (2013). Tuning of proportional retarded controllers: Theory and experiments. *IEEE Transactions on Control Systems Technology, 21*(3), 983–990.

Vyhlídal, T., Zítek, P., & Paulů, K. (2009). Design, modelling and control of the experimental heat transfer set-up. In J. J. Loiseau et al. (Ed.), *Topics in time delay systems. analysis, algorithms, and control*, *Lecture Notes in Control and Information Sciences* (Vol. 308, pp. 303–314). Springer.

Vyhlídal, T., Michiels, W., & McGahan, P. (2010). Synthesis of strongly stable state-derivative controllers for a time-delay system using constrained non-smooth optimization. *IMA Journal of Mathematical Control and Information, 27*(4), 437–455.

Zhou, B., Liu, Q., & Michiels, W. (2019). Design of pseudo-predictor feedback for neutral-type linear systems with both state and input delays. *Automatica, 109*, 108502.

Zhou, K., Doyle, J. C., & Glover, K. (1995). *Robust and optimal control*. Prentice Hall.